

**IN THE UNITED STATES DISTRICT COURT  
FOR THE EASTERN DISTRICT OF TEXAS  
SHERMAN DIVISION**

**TURBOCODE LLC,**

Plaintiff,

v.

**SIEMENS AKTIENGESELLSCHAFT,**

Defendant.

C.A. No. 4:24-cv-791

**JURY TRIAL DEMANDED**

**PATENT CASE**

**ORIGINAL COMPLAINT FOR PATENT INFRINGEMENT**

Plaintiff TurboCode LLC files this Original Complaint for Patent Infringement against Siemens AG, and would respectfully show the Court as follows:

**I. THE PARTIES**

1. Plaintiff TurboCode LLC (“TurboCode” or “Plaintiff”) is a Texas limited liability company with its address at 6000 Shepherd Mountain Cove, Suite #1604, Austin Texas 78730.

2. On information and belief, Defendant Siemens Aktiengesellschaft. (“Siemens” or “Defendant”) is a corporation organized and existing under the laws of Germany with a place of business at Werner-von-Siemens-Straße 1, 80333 Munich, Germany.

**II. JURISDICTION AND VENUE**

3. This action arises under the patent laws of the United States, Title 35 of the United States Code. This Court has subject matter jurisdiction of such action under 28 U.S.C. §§ 1331 and 1338(a).

4. On information and belief, Defendant is subject to this Court’s specific and general personal jurisdiction, pursuant to due process and the Texas Long-Arm Statute, due at least to its business in this forum, including at least a portion of the infringements alleged herein.

5. Without limitation, on information and belief, within this state, Defendant used the patented invention thereby committing, and continuing to commit, acts of patent infringement alleged herein. In addition, on information and belief, Defendant derived revenues from its infringing acts occurring within Texas. Further, on information and belief, Defendant is subject to the Court's general jurisdiction, including from regularly doing or soliciting business, engaging in other persistent courses of conduct, and deriving substantial revenue from goods and services provided to persons or entities in Texas. Further, on information and belief, Defendant is subject to the Court's personal jurisdiction at least due to its sale of products and/or services within Texas. Defendant committed such purposeful acts and/or transactions in Texas such that it reasonably should know and expect that it could be haled into this Court as a consequence of such activity.

6. Venue is proper in this district under 28 U.S.C. § 1400(b). On information and belief, from and within this District Defendant has committed at least a portion of the infringements at issue in this case.

7. For these reasons, personal jurisdiction exists and venue is proper in this Court under 28 U.S.C. § 1400(b).

**III. COUNT I**  
**(PATENT INFRINGEMENT OF UNITED STATES PATENT NO. 6,813,742)**

8. Plaintiff incorporates the above paragraphs herein by reference.

9. On November 2, 2004, the USPTO duly and legally issued U.S. Patent No. 6,813,742 ("the '742 Patent" or "Patent-in-Suit"), entitled "High Speed Turbo Codes Decoder for 3G Using Pipelined SISO Log-Map Decoders Architecture." The '742 patent was the subject of a reexamination request filed on July 13, 2006. An *Ex Parte* Reexamination Certificate was issued for the '742 patent on February 10, 2009. A true and correct copy of the '742 Patent with its *Ex Parte* Reexamination Certificate is attached hereto as Exhibit 1.

10. TurboCode is the assignee of all right, title, and interest in the '742 patent, including all rights to enforce and prosecute actions for infringement and to collect damages for all relevant times against infringers of the '742 Patent. Accordingly, TurboCode possesses the exclusive right and standing to prosecute the present action for infringement of the '742 Patent by Defendant.

11. This case generally relates to decoder architectures and processes for receiving and decoding data in communications devices.

12. **Direct Infringement.** Upon information and belief, Defendant directly infringed claim 6 of the '742 Patent in Texas, and elsewhere in the United States, by performing actions comprising using or performing the claimed method of iteratively decoding a plurality of sequences of received baseband signals by using and/or testing the products, devices, systems, and components of systems that comply with the 3G and/or 4G/LTE standards as disclosed in the 3<sup>rd</sup> Generation Partnership Project ("3GPP") Standard Specifications (releases 8-11) governing cellular wireless communications including, but not limited to, CP 1243-7 LTE US, SCALEANCE MUM853-1(A1), SCALANCE MUM856-1 (A1), SIMATIC RTU3041C, SIMATIC S-7 1200, RUGGEDCOM RX1400, Ruggedcom RM1224-NAM 4G Router, SITRANS FM MAG 8000, Scalance M874 Series, and Scalance M876 Series ("Accused Instrumentalities").

13. Claim 6 of the '742 Patent *Ex Parte* Reexamination Certificate states:

A method of iteratively decoding a plurality of sequences of received baseband signals, the method comprising:

providing an input buffer comprising at least three shift registers, for receiving an input signal and generating first, second, and third shifted input signals;

providing first and second soft decision decoders serially coupled in a circular circuit, wherein each decoder processes soft decision from the preceding decoder output data, and wherein the first decoder further receives the first and second shifted input signals from the input buffer and the second decoder further receives the third shifted input signal from the input buffer;

providing at least one memory module coupled to an output of each of the first and second soft decision decoders, wherein the output of the memory module associated with the second soft decision decoder is fed back as an input of the first soft decision decoder;

processing systematic information data and extrinsic information data using the maximum a posteriori (AP) probability algorithm, and/or logarithm approximation algorithm;

generating soft decision based on the maximum a posteriori (MAP) probability algorithm, and/or logarithm approximation algorithm;

weighing and storing soft decision information into the corresponding memory module;

performing, for a predetermined number of times, iterative decoding from the first to the last of multiple decoders, wherein an output from the last soft decision decoder is fed back as an input to the first soft decision decoder, then from the first to the second decoders, and propagate to the last decoder in a circular circuit.

14. The Accused Instrumentalities provided or performed a method of iteratively decoding a plurality of sequences of received baseband signals, as shown below by their compliance with the 3G and/or 4G/LTE standards disclosed in the 3GPP Standard Specifications:

Data sheet	6GK7243-7SX30-0XE0
product type designation	<p><b>CP 1243-7 LTE US</b></p> <p>Communications processor CP 1243-7 LTE US for Connection of SIMATIC S7-1200 to LTE network in American frequency band .</p>
	
<p><b>transfer rate</b></p>	
<p>transfer rate</p> <ul style="list-style-type: none"> <li>• for LTE transmission                             <ul style="list-style-type: none"> <li>— with downlink / maximum</li> <li>— with uplink / maximum</li> </ul> </li> </ul>	<p>42 Mbit/s</p> <p>5.76 Mbit/s</p>

(E.g., <https://mall.industry.siemens.com/mall/en/us/Catalog/DatasheetDownload?downloadUrl=teddatasheet%2F%3Fformat%3DPDF%26caller%3DMall%26mlfbs%3D6GK72437SX300XE0>)

[%26language%3Den\).](#)

<b>Detail</b>	
<b>Nominal size</b>	From DN 25 – 1200 (1" to 48") From DN 50 – 600 (1" – 24") for CT version under the MI001 and OIML R49 Class I & II
<b>Accuracy</b>	0.2% ± 2mm/s and 0.4% ± 2mm/s
<b>Input / output</b>	2 passive outputs
<b>Communication</b>	Local Modbus RTU IrDA (Infrared comm.), Modbus RS 232/485, Radio Encoder (Sensus Protocol), 4G LTE M/NB IoT

(E.g., <https://www.siemens.com/global/en/products/automation/process-instrumentation/flow-measurement/electromagnetic/sitrans-fm-mag-8000.html>).

## 3

## Description

## 3.1 Data transmission

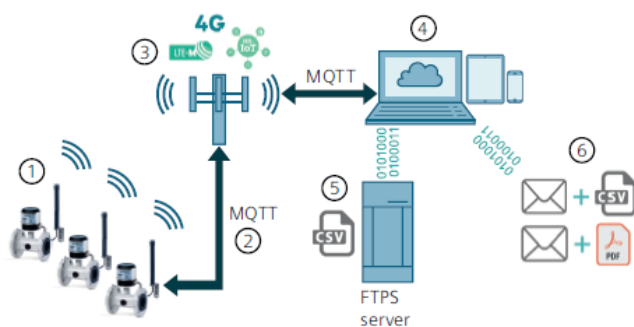
The Wireless Communication Module transmits information using a wireless network (4G/LTE, LTE-M, NB-IoT, 2G). Automatic network selection is possible.

Communication with users takes place through a industrial internet of things (IIoT) web application.

The Wireless Communication Module has the following capabilities:

- sending and receiving to a web interface
- sending measurement data (in csv file format) by email to the predefined email addresses or customer specified FTP server

The measurement data collected from MAG 8000 is stored in the Wireless Communication Module until it is fully transmitted. In case of a power or network failure the collected data is stored on the SD card in the Wireless Communication Module.



- | Pos. | Description  |
|------|--|
| ①    | MAG 8000 with Wireless Communication Module          |
| ②    | Message Queuing Telemetry Transport (MQTT)           |
| ③    | Mobile network                                       |
| ④    | Industrial internet of things (IIoT) web application |
| ⑤    | CSV file on FTPS server                              |
| ⑥    | Email with CSV or PDF file attached                  |

Figure 3-1 Data transmission

(E.g., [https://www.rskdatabasen.se/infoDocs/MAN/MAN\\_1202\\_5144228.pdf](https://www.rskdatabasen.se/infoDocs/MAN/MAN_1202_5144228.pdf)).

# SIEMENS

## Data sheet

**6GK5856-2EA10-3AA1**



SCALANCE MUM856-1 (A1) 5G router, rel. 16, IP65, for wireless IP communication from Ethernet-based applications via public 3/4/5G mobile radio networks and private 5G networks, VPN, firewall, NAT, IPv6, connection to SINEMA RC via CLP, 4 N-connect connections, 1x micro SIM slot, eSIM, 1x10/100/1000 Mbps M12 socket, redundant DC 24 V, M12 L-coded, PoE, -30...+70 °C, CLP slot, 1x DI and 1x DO, A-coded, observe national approvals!

transfer rate	
transfer rate / for Industrial Ethernet	10 Mbit/s, 100 Mbit/s, 1000 Mbit/s
transfer rate	
<ul style="list-style-type: none"> <li>• with UMTS transmission / with downlink / maximum</li> <li>• with UMTS transmission / with uplink / maximum</li> <li>• for LTE transmission / with downlink / maximum</li> <li>• for LTE transmission / with uplink / maximum</li> <li>• for 5G transmission / with downlink / maximum</li> <li>• for 5G transmission / with uplink / maximum</li> </ul>	<p>42 Mbit/s</p> <p>5.76 Mbit/s</p> <p>1000 Mbit/s</p> <p>200 Mbit/s</p> <p>1000 Mbit/s</p> <p>500 Mbit/s</p>
interfaces	

(E.g., <https://mall.industry.siemens.com/mall/en/ww/Catalog/DatasheetDownload?downloadUrl=teddatasheet%2F%3Fformat%3DPDF%26caller%3DMall%26mlfbs%3D6GK5856-2EA10-3AA1%26language%3Den>).

# SIEMENS

Data sheet

6GK5853-2EA10-2AA1



SCALANCE MUM853-1 (A1) 5G router, rel. 16, IP30, for wireless IP communication from Ethernet-based applications via public 3/4/5G mobile radio networks and private 5G networks, VPN, firewall, NAT, IPv6, connection to SINEMA RC via CLP, 4 SMA connections, 1x micro SIM slot, eSIM, 4x10/100/1000 Mbps RJ45 port, redundant DC 24 V, -30... +60 °C, CLP slot, 1x DI and 1x DO, observe national approvals!

transfer rate	
transfer rate / for Industrial Ethernet	10 Mbit/s, 100 Mbit/s, 1000 Mbit/s
transfer rate	
<ul style="list-style-type: none"> <li>• with UMTS transmission / with downlink / maximum</li> <li>• with UMTS transmission / with uplink / maximum</li> <li>• for LTE transmission / with downlink / maximum</li> <li>• for LTE transmission / with uplink / maximum</li> <li>• for 5G transmission / with downlink / maximum</li> <li>• for 5G transmission / with uplink / maximum</li> </ul>	<p>42 Mbit/s</p> <p>5.76 Mbit/s</p> <p>1000 Mbit/s</p> <p>200 Mbit/s</p> <p>1000 Mbit/s</p> <p>500 Mbit/s</p>

(E.g., <https://mall.industry.siemens.com/mall/en/ww/Catalog/DatasheetDownload?downloadUrl=teddatasheet%2F%3Fformat%3DPDF%26caller%3DMall%26mlfbs%3D6GK5853-2EA10-2AA1%26language%3Den>).





Siemens SCALANCE

## SCALANCE M874/M876 SERIES

### Mobile Wireless Routers

Siemens SCALANCE M874/M876 is a series of mobile wireless routers, both stationary and mobile stations can be connected to a central control and monitoring system via GSM (2G), UMTS (3G), or LTE (4G).

#### FEATURES

- High data rates allow the transmission of mass data or images in real time
- Provider independent
- Connection of extremely remote substations is possible

#### ORDERING INFORMATION

Article Number	Description
6GK5874-2AA00-2AA2	SCALANCE M874-2 2G router, for wireless IP communication from Ethernet-based automation devices via 2G mobile radio VPN, firewall, NAT, 2-port switch; 1x digital input, 1x digital output; observe national approvals!
6GK5874-3AA00-2AA2	SCALANCE M874-3 3G router, for the wireless IP communication from Ethernet-based Programmable controllers via 3G mobile radio HSPA+, VPN, Firewall, NAT, 2-port switch; 1x digital input, 1x digital output; observe national approvals!
6GK5876-3AA02-2BA2	SCALANCE M876-3 3G router, for the wireless IP communication of Ethernet-based Programmable controllers via 3G mobile radio HSPA+/EV-DO, VPN, Firewall, NAT 4-port switch; Antenna diversity; 1x digital input, 1x digital output; observe national approvals! Observe provider's approvals!
6GK5876-3AA02-2EA2	SCALANCE M876-3 3G router ROK, for wireless IP communication from Ethernet-based automation devices via 3G mobile radio optimized for use in Republic of Korea, HSPA+, VPN, Firewall, NAT, 4-port switch; Antenna diversity; 1x digital input, 1x digital output; observe national approvals!
6GK5876-4AA00-2BA2	SCALANCE M876-4 4G router, for the wireless IP communication from Ethernet-based Programmable controllers via LTE (4G) mobile radio optimized for use in Europe, VPN, Firewall, NAT, 4-port switch; 2x SMA antennas, MIMO Technology; 1x digital input, 1x digital output; observe national approvals!
6GK5876-4AA00-2DA2	SCALANCE M876-4 LTE (4G) NAM, for wireless IP communication from Ethernet-based automation devices via LTE (4G) mobile radio, optimized for use in North America, VPN, Firewall, NAT, 4-port switch; 2x SMA antennas, MIMO Technology; 1x digital input, 1x digital output; observe national approvals!

(E.g., <https://www.industrialcomms.com/products/scalance-m874-m876-series>).

RUGGEDCOM RX1400 | Technical data

## Technical data

**Serial**  
2 x RS232 / 422 / 485

**Ethernet**  
4 x 10/100 TX

**Pluggable optics**  
2 x SFP ports Gigabit / 100 FX

**Carrier**  
Dual SIM support

**Memory**  
Micro SD slot for application data storage

**Cellular connectivity**  
4G / 3G / 2G

**Wireless LAN**  
802.11 a/b/g/n

**GPS**  
GPS input for location data

**Relay**  
Failsafe relay form C

**Power supply**  
+/- 12-24 VDC (9 - 36 VDC)  
+/- 48 VDC (36-72 VDC)  
HI (88 - 264 VAC / 98 - 300 VDC)

**Management**  
Local serial console

SIEMENS RUGGEDCOM RX1400

88 mm

150 mm

S1

S2

S0

CONSOLE

SIM

ANT1

ANT2

ANT3

ANT4

ANT5

POWER

ALARM

CELL

12-24VDC 2-1A

g\_RCM0\_XX\_00034

(E.g., <https://assets.new.siemens.com/siemens/assets/api/uuid:7027e386-54c1-47ef-85c5-6a9f67d8a6dd/di-pa-ci-rugged-communication-rx1400-brochure-en.pdf>).

## Data sheet

6GK6108-4AM00-2DA2

product type designation



RM1224 LTE(4G) NAM

RUGGEDCOM RM1224-NAM 4G ROUTER For wireless IP-communication from Ethernet based devices via LTE(4G)- mobile radio, optimized for use in North America, VPN, firewall, NAT 4-port switch 2x SMA antenna Connectors, MIMO technology 1xdig. input, 1xdig. output Please note national approvals!

transfer rate	
transfer rate / for Industrial Ethernet	10 Mbit/s, 100 Mbit/s
transfer rate	
<ul style="list-style-type: none"> <li>• for GPRS transmission / with downlink / maximum</li> <li>• for GPRS transmission / with uplink / maximum</li> <li>• with eGPRS transmission / with downlink / maximum</li> <li>• with eGPRS transmission / with uplink / maximum</li> <li>• with UMTS transmission / with downlink / maximum</li> <li>• with UMTS transmission / with uplink / maximum</li> <li>• for LTE transmission / with downlink / maximum</li> <li>• for LTE transmission / with uplink / maximum</li> </ul>	85.6 kbit/s 85.6 kbit/s 236.8 kbit/s 236.8 kbit/s 14.4 Mbit/s 5.76 Mbit/s 100 Mbit/s 50 Mbit/s
WAN connection	
type of wireless network / is supported	LTE, UMTS, GSM
type of mobile wireless service / is supported	GPRS, eGPRS, HSPA+
operating frequency / for GSM transmission	850 MHz, 900 MHz, 1800 MHz, 1900 MHz
operating frequency / with UMTS transmission	850 MHz, AWS-1 (1700/2100) MHz, 1900 MHz
operating frequency / for LTE transmission	700 MHz, 850 MHz, AWS-1 (1700/2100) MHz, 1900 MHz

(E.g., <https://mall.industry.siemens.com/mall/en/ww/Catalog/DatasheetDownload?downloadUrl=teddatsheet%2F%3Fformat%3DPDF%26caller%3DMall%26mlfbs%3D6GK6108-4AM00-2DA2%26language%3Den>).

For all products of SIMATIC S7 automation solutions, it is possible to set up a maintenance access or transmit measured values to a control center via mobile communications.



LTE connections for all SIMATIC S7-based automation devices

(E.g., <https://assets.new.siemens.com/siemens/assets/api/uuid:a8ccbe10-f27a-4522-8bd7-2042e314e612/technical-article-automating-with-lte.pdf>).

### Communication

The SIMATIC S7-1200 is equipped with a variety of communication mechanisms:

- Integrated PROFINET IO Controller interface
- Communications module with PROFIBUS DP master interface
- Communications module with PROFIBUS DP slave interface
- GPRS module for connection to GSM/G mobile networks
- LTE module for communication in mobile networks of the 4th generation (long term evolution)
- Communications processor for connection to TeleControl Server Basic control center software control center software via Ethernet, and for safe communication via IP-based networks
- Communications processor for connection to control centers for telecontrol applications
- RF120C for connection to SIMATIC Ident systems
- Module SM1278 for connecting IO-Link sensors and actuators
- Point-to-point connection via communications modules or Communication Boards.

(E.g., <https://mall.industry.siemens.com/mall/en/WW/Catalog/Products/10045647?tree=CatalogTree>).

15. For example, each of the Accused Instrumentalities performed iterative decoding using at least the BCJR algorithm.

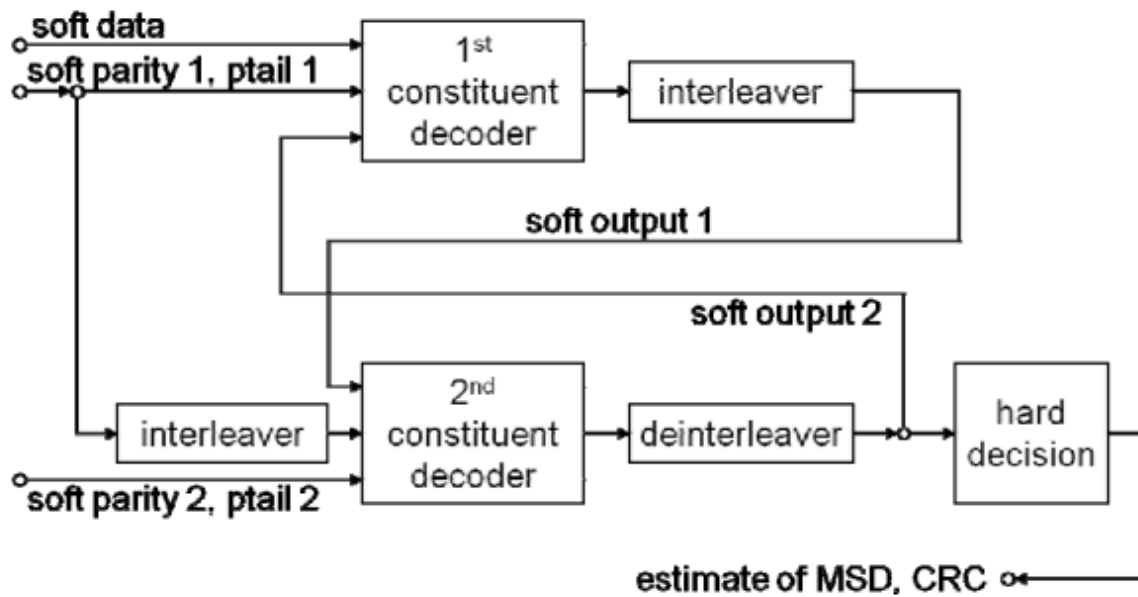


**Figure 18: Turbo decoder**

(See 3GPP TS 26.268 at 21 (v. 11), 17 (v. 8).)

See Mansour et al., “VLSI Architectures for SISO-APP Decoders,” IEEE Transactions On Very Large Scale Integration (“VLSI”) Systems, Vol. 11, No. 4 (Aug. 2003), at 627, *available at* <http://shanbhag.ece.illinois.edu/publications/mansr-tvlsi-2003-2.pdf>: “The BCJR algorithm was generalized in [S. Benedetto *et al.*, “A Soft-Input Soft-Output Maximum a posteriori (Map) Module to Decode Parallel and Serial Concatenated Codes,” JPL, TDA Progress Report 42-127, Nov. 1996] into a soft-input soft-output a posteriori probability (SISO- APP) algorithm to be used as a building block for iterative decoding in code networks with generic topologies...” *See also* Cheng *et al.* “A 0.077 to 0.168 nj/bit/iteration Scalable 3GPP LTE Turbo Decoder with an Adaptive Sub-Block Parallel Scheme and an Embedded DVFS Engine,” 2010 IEEE Custom Integrated Circuits Conference (CICC) (19-22 Sept. 2010), at 3, *available at* [13](https://dspace.mit.edu/bitstream/handle/1721.1/72198/Chandrakasan-</a></p>
</div>
<div data-bbox=)

[a%200.077%20to%200.168.pdf?sequence=1&isAllowed=y](#) (citation omitted): “Figure 3 shows the system architecture. The blocks in the dashed box handle the turbo decoding operations, and those outside the dashed box belong to the DVFS scheme. Turbo decoding is an iterative process with several turbo iterations. Each turbo iteration comprises two soft-in, soft-out (SISO) decoding processes using BCJR algorithm with the first one performed on the input code block in the original order and the second one in an order generated by the interleaver block.” *See also* “Digital cellular telecommunications system (Phase 2+); Universal Mobile Telecommunications System (UMTS); eCall data transfer; In-band modem solution; ANSI-C reference code (3GPP TS 26.268 version 11.0.0 Release 11),” at 14, *available at* [https://www.etsi.org/deliver/etsi\\_ts/126200\\_126299/126268/11.00.00\\_60/ts\\_126268v110000p.pdf](https://www.etsi.org/deliver/etsi_ts/126200_126299/126268/11.00.00_60/ts_126268v110000p.pdf) (“3GPP TS 26.268 v. 11”); “Digital cellular telecommunications system (Phase 2+); Universal Mobile Telecommunications System (UMTS); eCall data transfer; In-band modem solution; ANSI-C reference code (3GPP TS 26.268 version 8.0.0 Release 8),” at 17, *available at* [https://www.etsi.org/deliver/etsi\\_ts/126200\\_126299/126268/08.00.00\\_60/ts\\_126268v080000p.pdf](https://www.etsi.org/deliver/etsi_ts/126200_126299/126268/08.00.00_60/ts_126268v080000p.pdf) (“3GPP TS 26.268 v. 8”):

Type/Constant	Dimension	Description
/* Synchronization */		
const Int16 wakeupSin500	[16]	sine waveform at 500 Hz
const Int16 wakeupCos500	[16]	cosine waveform at 500 Hz
const Int16 wakeupSin800	[10]	sine waveform at 800 Hz
const Int16 wakeupCos800	[10]	cosine waveform at 800 Hz

*See also id.* at 20 (v. 11), 16-17 (v. 8) and source code release accompanying 3GPP TS 26.268, `ecall_fec.c`, lines 232-268:

```

/*=====*/
/* PSAP FUNCTION: PsapReceiver */
/*-----*/
/* Description: PSAP receiver function (decoding is done outside) */
/* */
/* In:      const ModState* ms      -> modulator struct */
/*          const Int16*   pcm      -> input data for demodulation */
/* Out:     IntLLR*         softBits <- demodulated soft bit sequence */
/*-----*/
void PsapReceiver(const ModState *ms, const Int16 *pcm, IntLLR *softBits)

/*=====*/
/* PSAP FUNCTION: SymbolDemod */
/*-----*/
/* Description: symbol demodulator */
/* */
/* In:      const ModState* ms      -> modulator struct */
/*          const Int16*   mPulse   -> received pulse train */
/* Out:     IntLLR*         softBits <- demodulated soft bit sequence */
/*-----*/
void SymbolDemod(const ModState *ms, const Int16 *mPulse, IntLLR *softBits)

```

(E.g., `ecall_fec.c` line 163 `Bool FecDecode(const IntLLR *in, Int16 rv, Ord1 *out)`).

```

/*=====*/
/* DECODER FUNCTION: FecDecode */
/*-----*/
/* Description: decoding to find the MSD */
/* */
/* In:      const IntLLR* in      -> received soft bits */
/*          Int16      rv      -> redundancy version */
/* Out:     Ord1*      out      <- decoded MSD in binary representation */
/* Return: Bool          <- result of CRC check */
/*-----*/
Bool FecDecode(const IntLLR *in, Int16 rv, Ord1 *out)

```

(E.g., `ecall_fec.c` line 240 `/*iterative decoding*/for (i = 0; i < FEC_ITERATIONS; i++)`).<sup>1</sup>

See also May et al., “A 150Mbit/s 3GPP LTE Turbo code decoder,” 2010 Design, Automation & Test in Europe Conference & Exhibition (March 8-12, 2010), available at <https://ieeexplore.ieee.org/document/5457035/authors#authors>: “3GPP long term evolution (LTE) enhances the wireless communication standards UMTS and HSDPA towards higher throughput.

---

<sup>1</sup> All citations to source code refer to the source code release accompanying 3GPP TS 26.268, available at <https://portal.3gpp.org/desktopmodules/Specifications/SpecificationDetails.aspx?specificationId=1446>.” Specific line citations for this and other source code are to the version accompanying Release 11, but substantially identical code is present in the version accompanying Release 8, available from the same hyperlink.

A throughput of 150 Mbit/s is specified for LTE using 2×2 MIMO. For this, highly punctured Turbo codes with rates up to 0.95 are used for channel coding, which is a big challenge for decoder design. This paper investigates efficient decoder architectures for highly punctured LTE Turbo codes. We present a 150 Mbit/s 3GPP LTE Turbo code decoder, which is part of an industrial SDR multi-standard baseband processor chip.”

16. Additionally, or alternatively, the relevant standards bodies, such as 3GPP, provided specifications that specify virtually all aspects of turbo encoders (*i.e.*, turbo-code transmitters), turbo decoders (*i.e.*, turbo-code receivers) and specify minimum performance requirements for the receivers and decoders (as well as encoders and transmitters) so that arbitrary transmitter-receiver pairs can communicate seamlessly. *See, e.g.*, ROHDE & SCHWARZ, “Radio fundamentals for cellular networks White paper,” 19 (Jan. 2019), *available at* [https://www.elektronikfokus.dk/wp-content/uploads/sites/5/WhitePaper\\_Radio-fundamentals-for-cellular-networks\\_wp\\_en\\_5216-0467-52\\_v0201.pdf](https://www.elektronikfokus.dk/wp-content/uploads/sites/5/WhitePaper_Radio-fundamentals-for-cellular-networks_wp_en_5216-0467-52_v0201.pdf).

17. On information and belief, each of the Accused Instrumentalities processed received baseband digital signals in an iterative manner. It was not commercially-feasible to implement turbo decoders in a non-iterative manner. No known commercial turbo decoder implementation used a pipeline of a SISO pair (with interleave/deinterleave operations) as replicated hardware blocks to fully replace iterations, and it is universally known in industry and academia that decoding of 3G/4G LTE turbo codes was explicitly and inherently iterative by both requirement and design. *See, e.g.*, Dejan Spasov, “Decoding of LTE Turbo Codes Initialized with the Two Recursive Convolutional Codes,” 2020 43rd International Convention on Information, Communication and Electronic Technology (MIPRO) (2020), *available at* <https://ieeexplore.ieee.org/document/9245282> (“Turbo codes were the first error-correcting codes

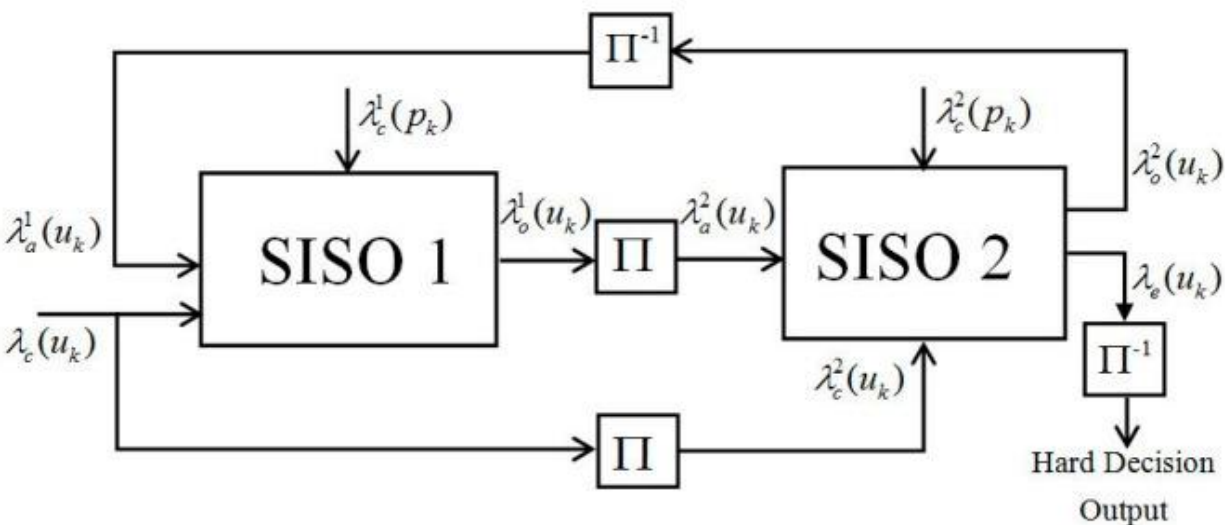


that demonstrated reliable communications near the channel capacity with practically feasible hardware. Due to their excellent error-correcting capability, they are part of many modern communication technologies, like 3G, 4G, LTE, etc. .... The decoding of LTE Turbo codes is iterative.”); Altera Corporation, “3GPP LTE Turbo Reference Design” (Jan. 2020), *available at* <https://www.intel.com/content/dam/www/programmable/us/en/pdfs/literature/an/an505.pdf> (“A Turbo decoder consists of two single soft-in soft-out (SISO) decoders, which work iteratively.”); Shuai Shao *et al.*, “Survey of Turbo, LDPC and Polar Decoder ASIC Implementations,” *IEEE Communications Surveys & Tutorials*, 1 (Jan. 17, 2019), *available at* [https://eprints.soton.ac.uk/427712/1/Survey\\_of\\_Turbo\\_LDPC\\_and\\_Polar\\_Decoder\\_ASIC\\_Implementations.pdf](https://eprints.soton.ac.uk/427712/1/Survey_of_Turbo_LDPC_and_Polar_Decoder_ASIC_Implementations.pdf) (“Both the turbo and LDPC codes employ an iterative decoding process, in which each successive attempt at decoding the information block informs the next, until the process converges to a legitimate codeword.”).

18. In iterative turbo decoder implementations, each iteration provides a decoding pass step. At each moment, a given error environment has an associated optimal number of decoding pass steps to produce the best results. Thus, a permanently-fixed number of decoding pass steps incurs either wasted computation or degraded performance. (*See, e.g.*, A. Matache *et al.*, “Stopping Rules for Turbo Decoders,” TMO Progress Report 42-142 (Aug. 15, 2000), *available at* [https://ipnpr.jpl.nasa.gov/progress\\_report/42-142/142J.pdf](https://ipnpr.jpl.nasa.gov/progress_report/42-142/142J.pdf)). Because the number of decoding pass steps can be arbitrary and dynamically varied, stopping rules (dependent on real-time computational measurements) are used to determine the number of decoding pass steps.

19. Were a non-iterative (pipeline) implementation employed, a fixed or maximum number of decoding pass steps would have to be implemented, with each decoding pass step requiring extensive hardware, and in practice yielding at almost every instant either too few stages

or too many stages. Thus, non-iterative implementations suffered disadvantages of higher costs, high power consumption, and lower average performance. In practice any commercial 4G LTE turbo decoder is necessarily recursive/iterative. While lower-level pipelines were employed in many hardware implementations of MAP computations *within* SISO elements, this is different in scope and method than a (non-iterative) pipeline of *full-scale SISO pair blocks* (with interleave/deinterleave operations) of replicated hardware to replace (SISO pair) iterations. All iterative implementations of 4G LTE turbo decoders were functionally equivalent to the figures below. The top of the figures below illustrates the feedback loop that forced 3G/4G LTE turbo decoders to be iterative. The iterative loop traversed elements SISO 1,  $\Pi$ , SISO 2,  $\Pi^{-1}$ , and closed with the signal path return to the input of SISO 1.



(E.g., see Jun Li et al., “Turbo Decoder Design based on an LUT-Normalized Log-MAP Algorithm,” Entropy (Basel) (Aug. 20, 2019), available at <https://www.ncbi.nlm.nih.gov/pmc/articles/PMC7515343/>).

20. Upon information and belief, the Accused Instrumentalities provided an input buffer comprising at least three shift registers, for receiving an input signal and generating first, second, and third shifted input signals. The Accused Instrumentalities provided (e.g., via an input

buffer) input to the constituent decoders of the turbo decoder. The input buffer comprised at least three shift registers. The input buffer received an input signal, and first, second, and third shifted input signals were generated for input to a turbo decoder. The generated first, second, and third shifted input signals, shown as “soft data,” “soft parity 1, ptail 1,” and “soft parity 2, ptail 2,” were input into the 1st constituent decoder and 2nd constituent decoder as shown below:

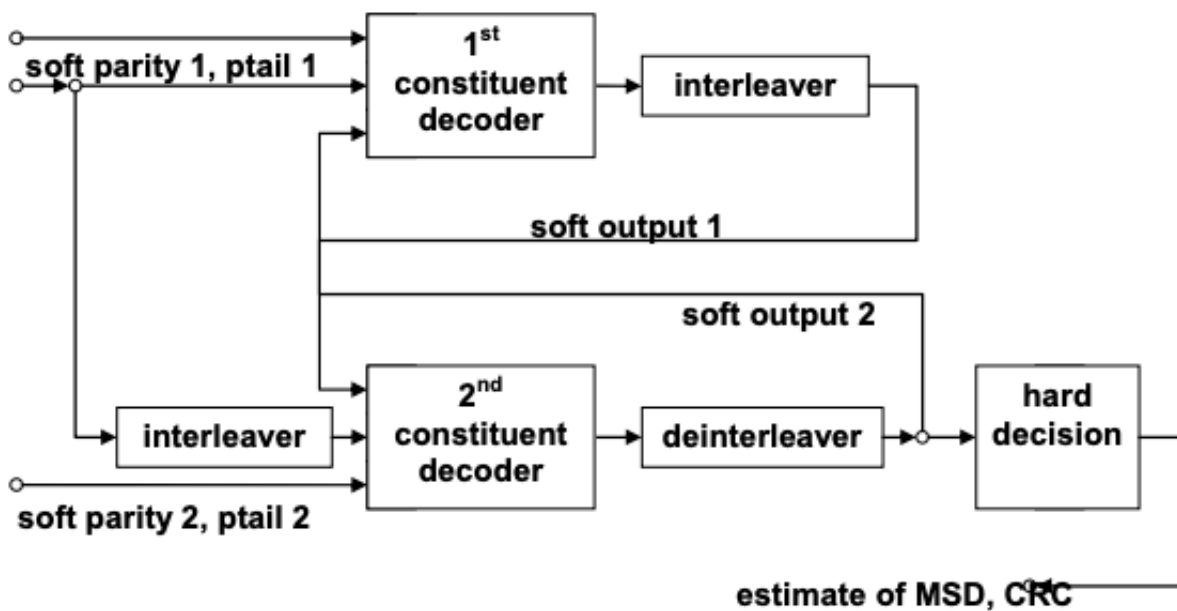


Figure 18: Turbo decoder

(E.g., 3GPP TS 26.267, at 14 (v. 11, v. 8)).

21. Upon information and believe, in the Accused Instrumentalities, each such buffer provided three sections based on operations of a turbo encoder. For example, an input buffer is denoted as Figure 7, labeled as a “channel coded bit buffer.”



**Figure 7: Channel coded bit buffer**

(See 3GPP TS 26.267, at 14 (v. 11, v. 8)). Note that the “soft data” of Figure 18 corresponds to the “MSD+CRC,” “tail 1,” and “tail 2” fields of Figure 7. Such a channel coded bit buffer could then be decoded using shifting to generate the first, second, and third shifted input signals, which were stored in registers for input into the turbo decoder: “6.1.3 Modulation: The encoded binary data stream bits  $b_i$  are grouped into symbols. Each symbol  $d_j$  carries 4 bits of information and modulates one basic downlink waveform... Table 4 describes the symbol modulation mapping between symbol and the downlink waveform. The downlink waveform is derived from the basic downlink waveform  $p_{DL}(n)$  by a cyclic right-shift by  $k$  samples, denoted by  $(p \rightarrow k)$ , and multiplication with a sign  $q$ .” (See 3GPP TS 26.267, at 22 (v. 11), 21 (v. 8)). See also Cheng et. al. “A 0.077 to 0.168 nj/bit/iteration Scalable 3GPP LTE Turbo Decoder with an Adaptive Sub-Block Parallel Scheme and an Embedded DVFS Engine,” 2010 IEEE Custom Integrated Circuits Conference (CICC) (19-22 Sept. 2010), at Fig. 3, available at <https://dspace.mit.edu/bitstream/handle/1721.1/72198/Chandrakasan-a%200.077%20to%200.168.pdf?sequence=1&isAllowed=y>:

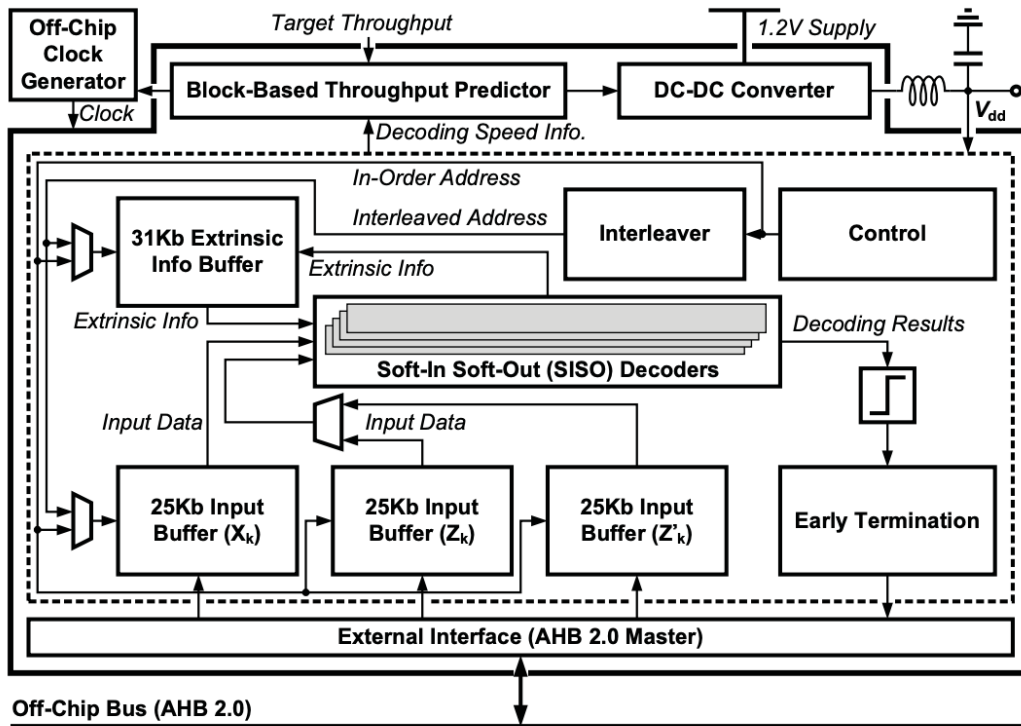


Fig. 3. The system architecture.

See also 3GPP TS 26.268 at 21 (v. 11), 17 (v. 8) and source code release accompanying 3GPP TS 26.268 ecall\_fec.c line 200 `void UpdateBuffer(IntLLR *chLLRbuffer, const IntLLR *softInBits, Int16 rv)` ecall\_fec.c line 225 `void DecodeBuffer(const IntLLR *syst1, const IntLLR *syst2, const IntLLR *parity1, const IntLLR *parity2, Ord1 *decBits)`.

22. Additionally, and alternatively, as discussed above, each of the Accused Instrumentalities processed received baseband digital signals in an iterative manner through its implementation of turbo decoding. Any turbo decoder implementation receiving and operating on an incoming input signal included an input buffer structure and three component shift registers to provide time-aligned values (*i.e.*, first, second, and third shifted input signals) needed for each SISO computation. To the extent that any of the Accused Instrumentalities did not implement shift register functions in hardware, it was a well-established convention to implement shift register functions via software. See, *e.g.*, Wikipedia, "Shift register," available at

[https://en.wikipedia.org/wiki/Shift\\_register](https://en.wikipedia.org/wiki/Shift_register) (“Many computer languages include instructions to ‘shift right’ and ‘shift left’ the data in a register, effectively dividing by two or multiplying by two for each place shifted.”); GeeksforGeeks, “Left Shift and Right Shift Operators in C/C++,” available at <https://www.geeksforgeeks.org/left-shift-right-shift-operators-c-cpp/>; mbedded.ninja, “Shift Registers,” §5 (Apr. 8, 2020), available at <https://blog.mbedded.ninja/electronics/components/shift-registers/>.

23. Upon information and belief, the Accused Instrumentalities provided first and second soft decision decoders serially coupled in a circular circuit, wherein each decoder processed soft decision from the preceding decoder output data, and wherein the first decoder further received the first and second shifted input signals from the input buffer and the second decoder further received the third shifted input signal from the input buffer.

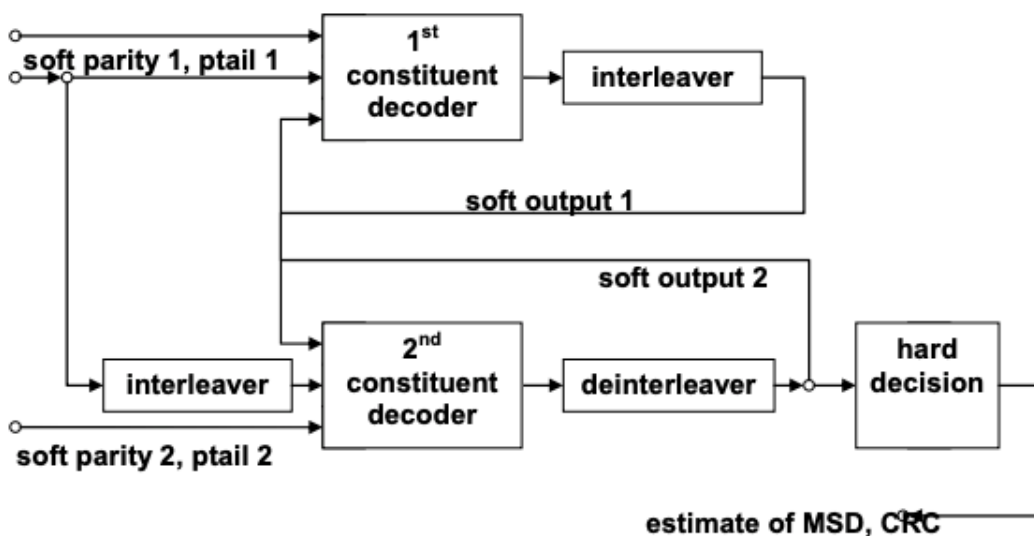


Figure 18: Turbo decoder

(E.g., 3GPP TS 26.267, at 14 (v. 11, v. 8)).

24. In the example, the first soft decision decoder output soft decision that became “soft output 1” after exiting “interleaver.” This “soft output 1” was fed as input into the second soft

decision decoder, “2nd constituent decoder,” for the second decision decoder to process. The second soft decision decoder also received the “soft parity 2, ptail 2” input signal. The second soft decision decoder output soft decision that became “soft output 2” after exiting “deinterleaver.” This “soft output 2” was fed as input into the first soft decision decoder for the first soft decision decoder to process. The first soft decision decoder, “1st constituent decoder,” also received the “soft data” and “soft parity 1, ptail 1” input signals. *See also Cheng et. al.* “A 0.077 to 0.168 nj/bit/iteration Scalable 3GPP LTE Turbo Decoder with an Adaptive Sub-Block Parallel Scheme and an Embedded DVFS Engine,” 2010 IEEE Custom Integrated Circuits Conference (CICC) (19-22 Sept. 2010), at 3, available at <https://dspace.mit.edu/bitstream/handle/1721.1/72198/Chandrakasan-a%200.077%20to%200.168.pdf?sequence=1&isAllowed=y> (citation removed): “Figure 3 shows the system architecture. The blocks in the dashed box handle the turbo decoding operations, and those outside the dashed box belong to the DVFS scheme. Turbo decoding is an iterative process with several turbo iterations. Each turbo iteration comprises two soft-in, soft-out (SISO) decoding processes using BCJR algorithm with the first one performed on the input code block in the original order and the second one in an order generated by the interleaver block.” *See also Valenti et al.*, “UMTS Turbo Code and an Efficient Decoder,” *International Journal of Wireless Information Networks*, Vol. 8, No. 4 (Oct. 2001), at 206, available at <https://community.wvu.edu/~mcvalenti/documents/valenti01.pdf> at Page 206, section 5. THE MAX\* OPERATOR, 5.1. Log-MAP Algorithm, 5.2. Max-log-MAP Algorithm.

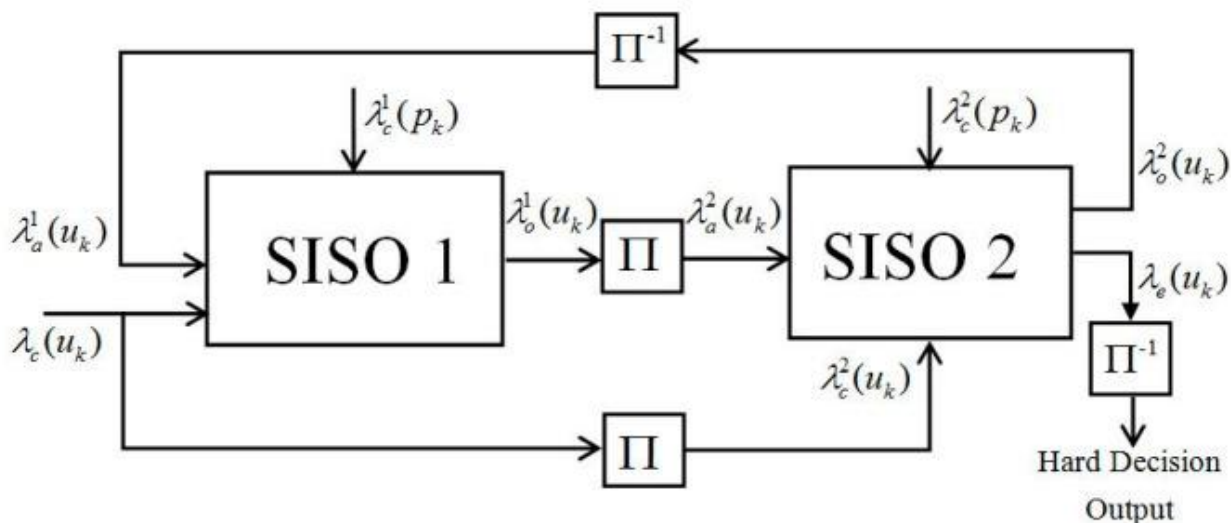
```

/*-----*/
/* DECODER FUNCTION: Bcjr */
/*-----*/
/* Description: BCJR algorithm */
/*-----*/
/* In:      const IntLLR* parity      -> received parity soft bits */
/* InOut:   IntLLR*      extrinsic  <-> extrinsic information */
/*-----*/
void Bcjr(const IntLLR *parity, IntLLR *extrinsic)

```

(E.g., 3GPP TS 26.268 at 21 (v. 11), 17 (v. 8)).

25. Additionally or alternatively, as explained above, all known commercial implementations of 4G LTE turbo decoders were iterative and functionally equivalent to the figures below. The figures below illustrate soft decision from the preceding decoder output (a posteriori information) being fed as an input (a priori information) in an iterative mode. The top of the figures below illustrates the feedback loop that forced 3G/4G LTE turbo decoders to be iterative. The iterative loop traversed elements SISO 1,  $\Pi$ , SISO 2,  $\Pi^{-1}$ , and closed with the signal path return to the input of SISO 1 to form a circular circuit.



See Jun Li et al., "Turbo Decoder Design based on an LUT-Normalized Log-MAP Algorithm," Entropy (Basel) (Aug. 20, 2019), available at <https://www.ncbi.nlm.nih.gov/pmc/articles/PMC7515343/> ("The SISO decoder consists of three input ports, which are system



information  $\lambda_c(u_k)$ , parity information  $\lambda_c(p_k)$ , and a priori information  $\lambda_a(u_k)$  which is computed by another SISO decoder. Two output ports of the SISO decoder generate external information  $\lambda_e(u_k)$  and posteriori information  $\lambda_o(u_k)$ . The different superscripts represent information corresponding to different SISO decoders, and subscript  $k$  denotes  $k$ -th bit information of the current variable.”).

26. As explained above, each of the Accused Instrumentalities processed received baseband digital signals in an iterative manner through its implementation of turbo decoding. Any turbo decoder implementation receiving and operating on an incoming input signal included an input buffer structure and three component shift registers to provide time-aligned values (*i.e.*, first, second, and third shifted input signals) needed for each SISO computation. To the extent that any of the Accused Instrumentalities did not implement shift register functions in hardware, it was a well-established convention to implement shift register functions via software. *See, e.g.*, Wikipedia, “Shift register,” available at [https://en.wikipedia.org/wiki/Shift\\_register](https://en.wikipedia.org/wiki/Shift_register) (“Many computer languages include instructions to 'shift right' and 'shift left' the data in a register, effectively dividing by two or multiplying by two for each place shifted.”); GeeksforGeeks, “Left Shift and Right Shift Operators in C/C++,” available at <https://www.geeksforgeeks.org/left-shift-right-shift-operators-c-cpp/>; mbedded.ninja, “Shift Registers,” §5 (Apr. 8, 2020), available at <https://blog.mbedded.ninja/electronics/components/shift-registers/>.

27. Upon information and belief, the Accused Instrumentalities provided at least one memory module coupled to an output of each of the first and second soft decision decoders, wherein the output of the memory module associated with the second soft decision decoder was fed back as an input of the first soft decision decoder. For example, the Accused Instrumentalities included at least one memory module (*e.g.*, “interleaver” to the right of the “1st constituent

decoder” and “deinterleaver” in the figures below), that was electrically coupled to an output of a corresponding soft decision decoder (e.g., “1st constituent decoder” and “2nd constituent decoder”), wherein the output of the memory module associated with the second soft decision decoder (“deinterleaver”) was fed back as an input of the first soft decision decoder, as shown below:

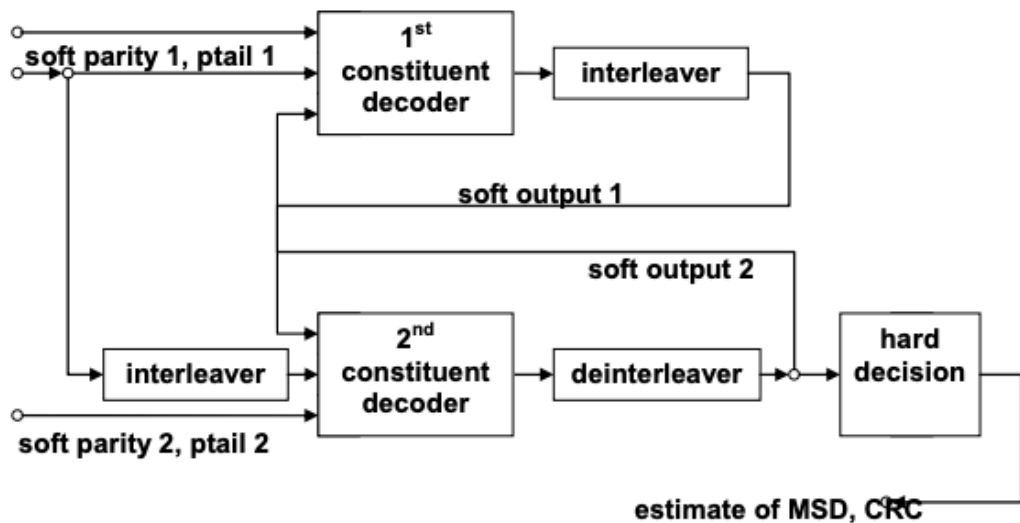


Figure 18: Turbo decoder

(E.g., 3GPP TS 26.267, at 25 (v. 11), 24 (v. 8)).

28. In the example, the “deinterleaver” memory module was associated with the second soft decision decoder, “2nd constituent decoder.” The output of the deinterleaver, “soft output 2,” was fed back as an input of the first soft decision decoder, “1st constituent decoder.” Additional evidence that the “interleaver” and “deinterleaver” comprised memory modules is shown in source code associated with the figure:

```

/* initialize memory */
Le12 = (IntLLR*)&decBits[0];
Le21 = (IntLLR*)&decBits[sizeof(IntLLR)*(NRB_INFO_CRC + NRB_TAIL)];

memset(Le12, 0, sizeof(IntLLR)*(NRB_INFO_CRC + NRB_TAIL));
memset(Le21, 0, sizeof(IntLLR)*(NRB_INFO_CRC + NRB_TAIL));

/* iterative decoding */
for (i = 0; i < FEC_ITERATIONS; i++) {
    memcpy(Le12, Le21, sizeof(IntLLR)*(NRB_INFO_CRC + NRB_TAIL));

    /* add received systematic bits to extrinsic information */
    for (j = 0; j < NRB_INFO_CRC+NRB_TAIL; j++) {
        temp = (Int32)Le12[j] + (Int32)syst1[j];
        Le12[j] = (ABS(temp) < LLR_MAX) ?
            (IntLLR)temp : (IntLLR)(SIGN(temp)*LLR_MAX);
    }
    /* decode code one (produces Le12) */
    Bcjr(parity1, Le12);

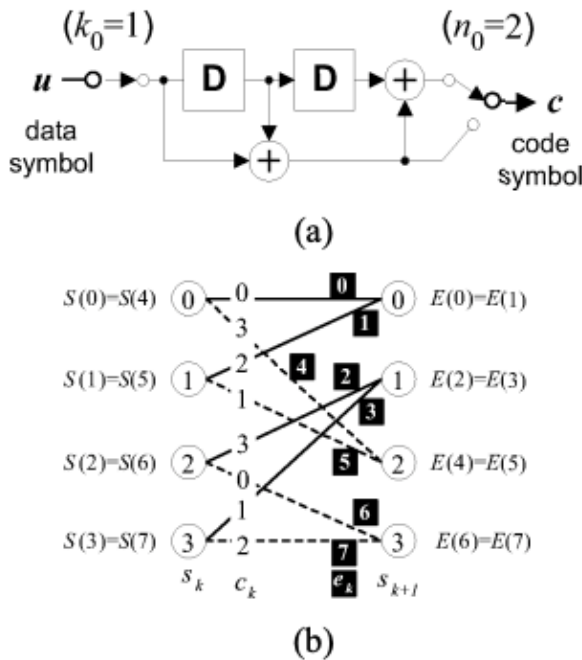
    /* interleave extrinsic information (produces interleaved Le12) */
    Interleave(Le12, Le21);

    /* add received systematic bits to extrinsic information */
    for (j = 0; j < NRB_INFO_CRC; j++) {
        temp = (Int32)Le21[j] + (Int32)syst1[interleaverSeq[j]];
        Le21[j] = (ABS(temp) < LLR_MAX) ?
            (IntLLR)temp : (IntLLR)((SIGN(temp))*LLR_MAX);
    }
    for (j = 0; j < NRB_TAIL; j++) {
        Le21[j+NRB_INFO_CRC] = syst2[j];
    }
    /* decode code two (produces interleaved Le21) */
    Bcjr(parity2, Le21);

    /* deinterleave extrinsic information (produces Le21) */
    Deinterleave(Le21);
}

```

(E.g., source code release accompanying 3GPP TS 26.268, `ecall_fec.c`, lines 232-268). See also Mansour et al., “VLSI Architectures for SISO-APP Decoders,” *IEEE Transactions On Very Large Scale Integration (“VLSI”) Systems*, Vol. 11, No. 4 (Aug. 2003) “Fig. 1. A (2, 1, 3) convolutional code. (a) An encoder with 2 memory delay elements (D) and modulo 2 adders, data symbol alphabet {0, 1}, code symbol alphabet {0, 1, 2, 3}, memory states {0, 1, 2, 3}, and code rate  $R = (1=2)$ . (b) A trellis section where solid edges correspond to  $u = 0$ , and dashed edges correspond to  $u = 1$ . The output code symbols  $c$  are shown on the edges. The edges are numbered with black squares, and the edge starting and ending states are shown on the left and right, respectively.” See also *id.* at FIG. 1:



See also Valenti et al., “UMTS Turbo Code and an Efficient Decoder,” *International Journal of Wireless Information Networks*, Vol. 8, No. 4 (Oct. 2001), at 207, available at <https://community.wvu.edu/~mcvalenti/documents/valenti01.pdf>: “Two key observations should be pointed out before going into the details of the algorithm: (1) It does not matter whether the

forward sweep or the reverse sweep is performed first; and (2) while the partial path metrics for the entire first sweep (forward or backward) must be stored in memory, they do not need to be stored for the entire second sweep. This is because the LLR values can be computed during the second sweep, and thus partial path metrics for only two stages of the trellis (the current and previous stages) must be maintained during the second sweep.” See also Cheng et. al. “A 0.077 to 0.168 nj/bit/iteration Scalable 3GPP LTE Turbo Decoder with an Adaptive Sub-Block Parallel Scheme and an Embedded DVFS Engine,” 2010 IEEE Custom Integrated Circuits Conference (CICC) (19-22 Sept. 2010), at Fig. 3, available at <https://dspace.mit.edu/bitstream/handle/1721.1/72198/Chandrakasan-a%200.077%20to%200.168.pdf?sequence=1&isAllowed=y>:

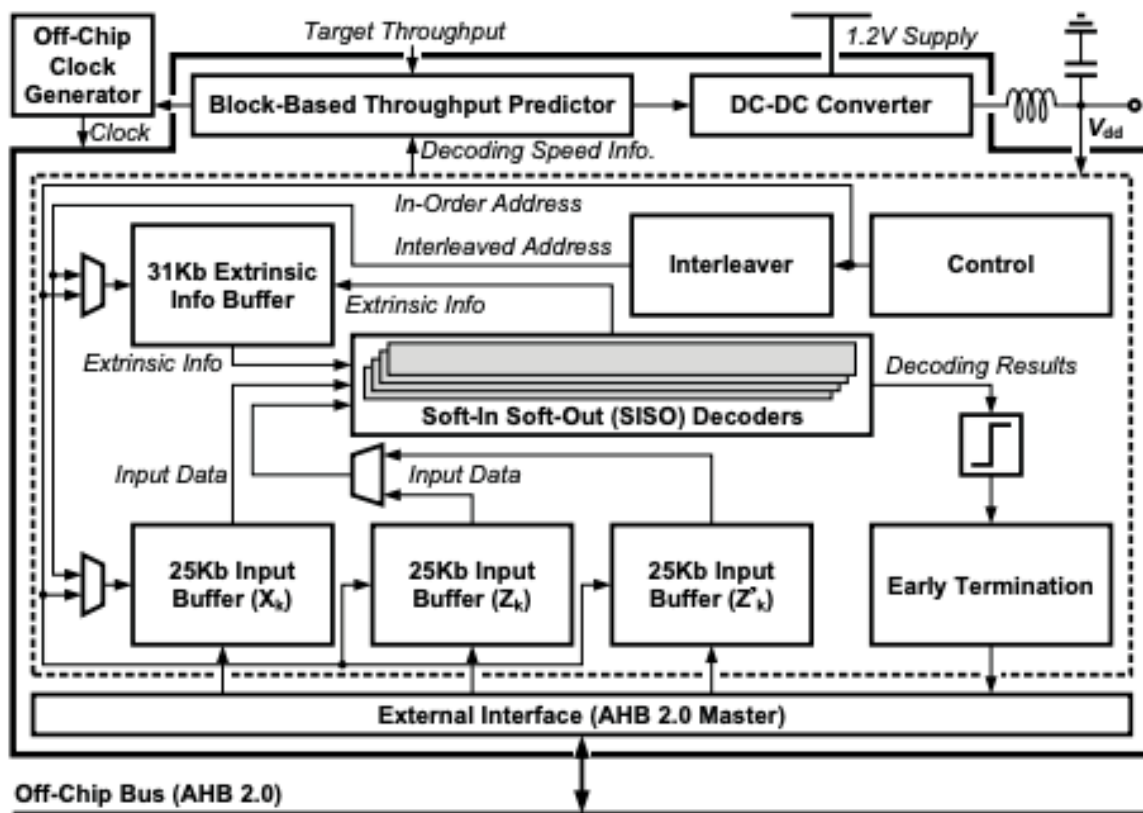


Fig. 3. The system architecture.

See also, source code release accompanying 3GPP TS 26.268, ecall\_fec.c, lines 232-268:

ecall\_fec.c line 232

```
/* initialize memory */
```

```
Le12 = (IntLLR*)&decBits[0];
```

```
Le21 = (IntLLR*)&decBits[sizeof(IntLLR)*(NRB_INFO_CRC + NRB_TAIL)];
```

```
memset(Le12, 0, sizeof(IntLLR)*(NRB_INFO_CRC + NRB_TAIL));
```

```
memset(Le21, 0, sizeof(IntLLR)*(NRB_INFO_CRC + NRB_TAIL));
```

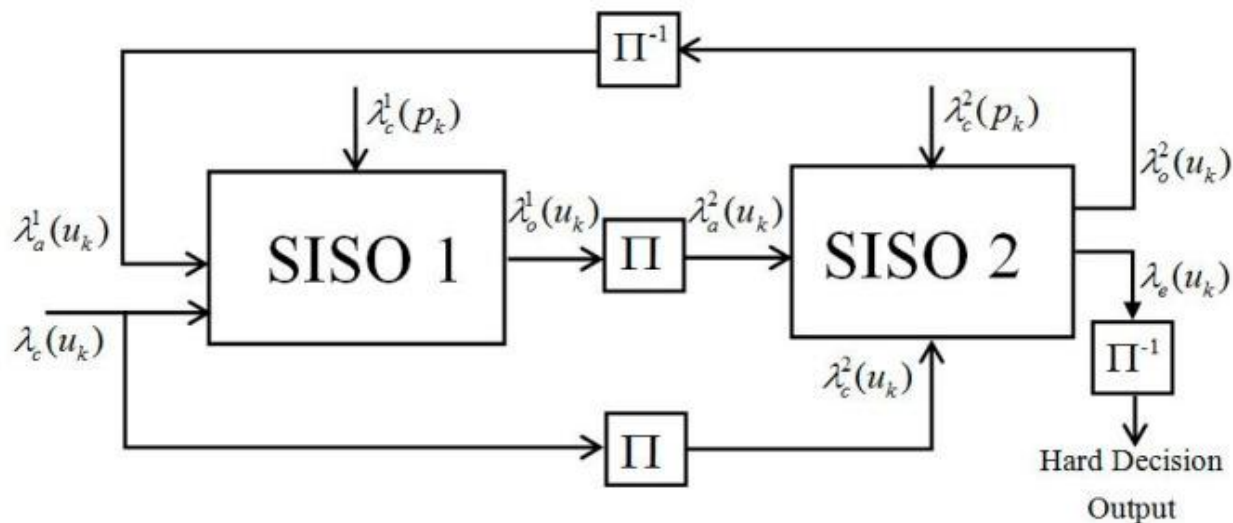
ecall\_fec.c line 250

```
Bcjr(parity1, Le12); /*corresponding memory module Le12*/
```

ecall\_fec.c line 265

```
Bcjr(parity2, Le21); /*corresponding memory module Le21*/
```

29. Additionally, or alternatively, as explained above, all known commercial implementations of 4G LTE turbo decoders were iterative and functionally equivalent to the figures below. The figures below illustrate output of the memory module associated with a last soft decision decoder fed back as an input to the first soft decision decoder via interleaving and/or de-interleaving (e.g., the a posteriori output of SISO 2 was de-interleaved with the associated memory module and fed back as a priori input of SISO 1).



See Jun Li et al., “Turbo Decoder Design based on an LUT-Normalized Log-MAP Algorithm,” Entropy (Basel) (Aug. 20, 2019), available at <https://www.ncbi.nlm.nih.gov/pmc/articles/PMC7515343/> (“Π and Π<sup>-1</sup> denote interleaving and de-interleaving, respectively.”).

30. Upon information and belief, the Accused Instrumentalities processed systematic information data and extrinsic information data using the maximum a posteriori (MAP) probability algorithm, and/or logarithm approximation algorithm. For example, the Accused Instrumentalities used at least the BCJR algorithm for turbo decoding in accordance with the figures below:

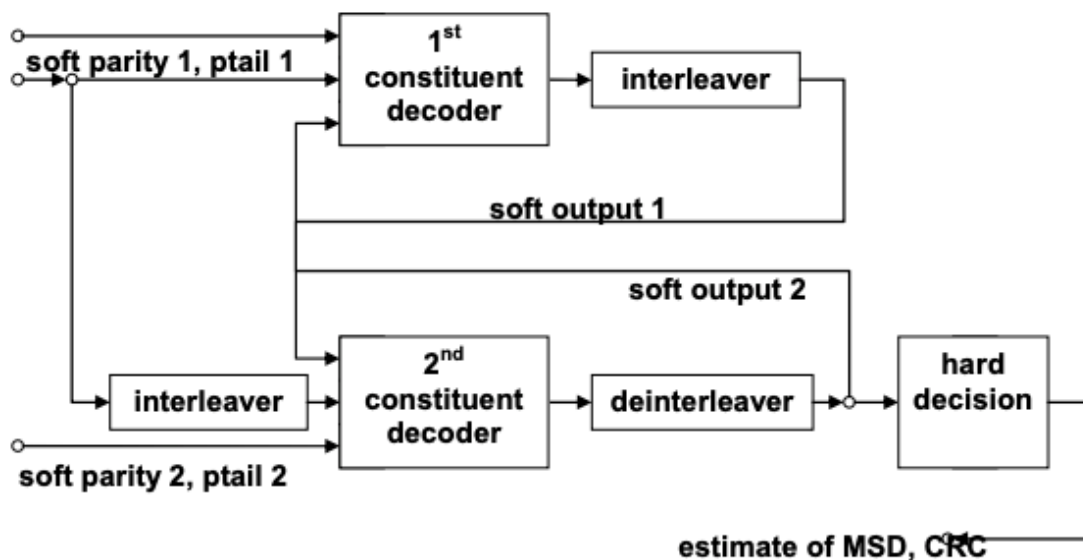


Figure 18: Turbo decoder

(E.g., 3GPP TS 26.267, at 25 (v. 11), 24 (v. 8)).

31. The source code associated with the figure indicates that it processes systematic information data and extrinsic information data using the BCJR algorithm:

```

/* initialize memory */
Le12 = (IntLLR*)&decBits[0];
Le21 = (IntLLR*)&decBits[sizeof(IntLLR)*(NRB_INFO_CRC + NRB_TAIL)];
memset(Le12, 0, sizeof(IntLLR)*(NRB_INFO_CRC + NRB_TAIL));
memset(Le21, 0, sizeof(IntLLR)*(NRB_INFO_CRC + NRB_TAIL));

/* iterative decoding */
for (i = 0; i < FEC_ITERATIONS; i++) {
    memcpy(Le12, Le21, sizeof(IntLLR)*(NRB_INFO_CRC + NRB_TAIL));

    /* add received systematic bits to extrinsic information */
    for (j = 0; j < NRB_INFO_CRC+NRB_TAIL; j++) {
        temp = (Int32)Le12[j] + (Int32)syst1[j];
        Le12[j] = (ABS(temp) < LLR_MAX) ?
            (IntLLR)temp : (IntLLR)(SIGN(temp)*LLR_MAX);
    }
    /* decode code one (produces Le12) */
    Bcjr(parity1, Le12);

    /* interleave extrinsic information (produces interleaved Le12) */
    Interleave(Le12, Le21);

    /* add received systematic bits to extrinsic information */
    for (j = 0; j < NRB_INFO_CRC; j++) {
        temp = (Int32)Le21[j] + (Int32)syst1[interleaverSeq[j]];
        Le21[j] = (ABS(temp) < LLR_MAX) ?
            (IntLLR)temp : (IntLLR)((SIGN(temp))*LLR_MAX);
    }
    for (j = 0; j < NRB_TAIL; j++) {
        Le21[j+NRB_INFO_CRC] = syst2[j];
    }

    /* decode code two (produces interleaved Le21) */
    Bcjr(parity2, Le21);

    /* deinterleave extrinsic information (produces Le21) */
    Deinterleave(Le21);
}

```

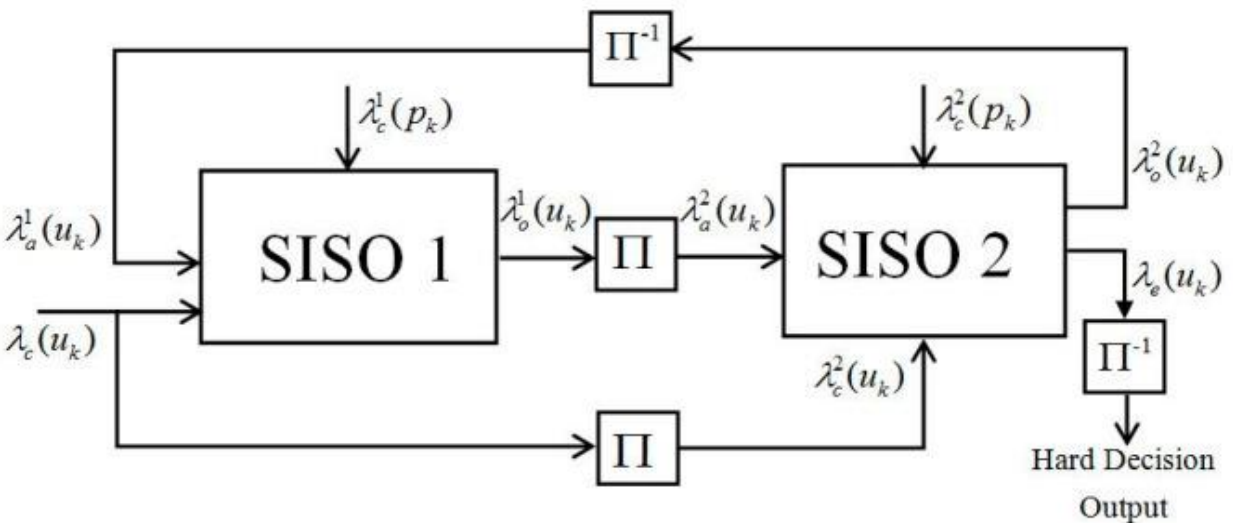
(E.g., see, source code release accompanying 3GPP TS 26.268, ecall\_fec.c, lines 232-268).



32. The BCJR algorithm is a MAP probability algorithm that processes systematic information data and extrinsic information data: “Turbo codes are composed of an interconnection of component codes through interleavers, typically convolutional codes, and their decoders consist of an equal number of component decoders each of which operates on its corresponding codeword and shares information with other component decoders iteratively according to the topology of the encoder. The decoding algorithm in the component decoders is the maximum a-posteriori probability (MAP) algorithm typically implemented in the form known as the Bahl–Cocke–Jelinek–Raviv (BCJR) algorithm. The main advantage of a MAP decoding algorithm over a maximum likelihood decoding algorithm such as the Viterbi algorithm is that it produces optimum soft information which is crucial to the operation of these decoders. The BCJR algorithm was generalized in [S. Benedetto *et al.*, “A Soft-Input Soft-Output Maximum a posteriori (Map) Module to Decode Parallel and Serial Concatenated Codes,” JPL, TDA Progress Report 42-127, Nov. 1996.] into a soft-input soft-output a posteriori probability (SISO-APP) algorithm to be used as a building block for iterative decoding in code networks with generic topologies. The advantages of the SISO-APP algorithm over other forms of the MAP algorithm is that it is independent of the code type (systematic/nonsystematic, recursive/nonrecursive, trellis with multiple edges), and it generates reliability information for code symbols as well as message symbols which makes it applicable irrespective of the concatenation scheme (parallel/serial/hybrid), and hence will be considered in this paper.” See Mansour et al., “VLSI Architectures for SISO-APP Decoders,” IEEE Transactions On Very Large Scale Integration (“VLSI”) Systems, Vol. 11, No. 4 (Aug. 2003), at 627, *available at* <http://shanbhag.ece.illinois.edu/publications/mansr-tvlsi-2003-2.pdf> (citations removed). See also

*id.* at 629 (“The decoding problem can now be defined as follows: given a noisy version of  $\underline{c}$  denoted by  $\underline{y}=\Delta(y_1, \dots, y_k, \dots, y_L)$ , find the data sequence  $\underline{u}$ . There are two probabilistic solutions to this decoding problem. Maximum likelihood (ML) decoding determines the most likely connected path  $\underline{s}$  through the trellis that maximizes the probability  $P(\underline{y}|\underline{s})$ . From  $\underline{s}$ , the most likely data sequence  $\underline{u}$  is easily determined using (1). On the other hand, MAP decoding, which we consider here, determines  $\underline{u}$  by estimating each of the symbols  $u_k$  independently using the observations  $\underline{y}$ . The  $k$ th estimated symbol  $u_k$  is the one that maximizes the posterior probability  $P(u_k|\underline{y})$ , and hence the name symbol-by-symbol MAP. The SISO-APP algorithm, a generalized version of the BCJR-APP algorithm, is a probabilistic algorithm that solves the MAP decoding problem.”) (citations removed).

33. Additionally, or alternatively, as explained above, all known commercial implementations of 4G LTE turbo decoders were iterative and functionally equivalent to the figures below. The figures below illustrate that each decoder processed systemic information data and extrinsic information data—system information  $\lambda_c(u_k)$ , parity information  $\lambda_c(p_k)$ , a priori information  $\lambda_a(u_k)$  and external information  $\lambda_e(u_k)$ :



See Jun Li et al., "Turbo Decoder Design based on an LUT-Normalized Log-MAP Algorithm," Entropy (Basel) (Aug. 20, 2019), available at <https://www.ncbi.nlm.nih.gov/pmc/articles/PMC7515343/>. See also, e.g., Guohui Wang et al., "High-throughput Contention-Free Concurrent Interleaver Architecture for Multi-standard Turbo Decoder," ASAP 2011—22nd IEEE International Conference on Application-specific Systems, Architectures and Processors 113 (Sept. 2011); Cristian Anghel et al., "CTC Turbo Decoding Architecture for LTE Systems Implemented on FPGA," ICN 2012: The Eleventh International Conference on Networks 199, 199-200 (2012).

34. Each soft decision decoder on all known commercial implementations of any turbo decoder processed systematic information data and extrinsic information data using a maximum a posteriori (MAP) probability algorithm and/or a logarithm approximation algorithm to yield posteriori information  $\lambda_o(u_k)$ . See Jun Li et al., "Turbo Decoder Design based on an LUT-Normalized Log-MAP Algorithm," Entropy (Basel) (Aug. 20, 2019), available at <https://www.ncbi.nlm.nih.gov/pmc/articles/PMC7515343/> (discussing use of a log maximum a posteriori decoding algorithm). See also, e.g., Guohui Wang et al., "High-throughput Contention-Free Concurrent Interleaver Architecture for Multi-standard Turbo Decoder," ASAP 2011—22nd IEEE International Conference on Application-specific Systems, Architectures and Processors 113 (Sept. 2011) (noting that MAP decoders are used as the component SISO decoders); Cristian Anghel et al., "CTC Turbo Decoding Architecture for LTE Systems Implemented on FPGA," ICN 2012: The Eleventh International Conference on Networks 199, 200 (2012) (describing ideal use of classic MAP algorithm and practical implementation of log-MAP algorithms).

35. Upon information and belief, the Accused Instrumentalities generated soft decision based on the maximum a posteriori (MAP) probability algorithm and/or logarithm approximation algorithm. For example, the Accused Instrumentalities used at least the BCJR algorithm for decoding in accordance with the figures below:

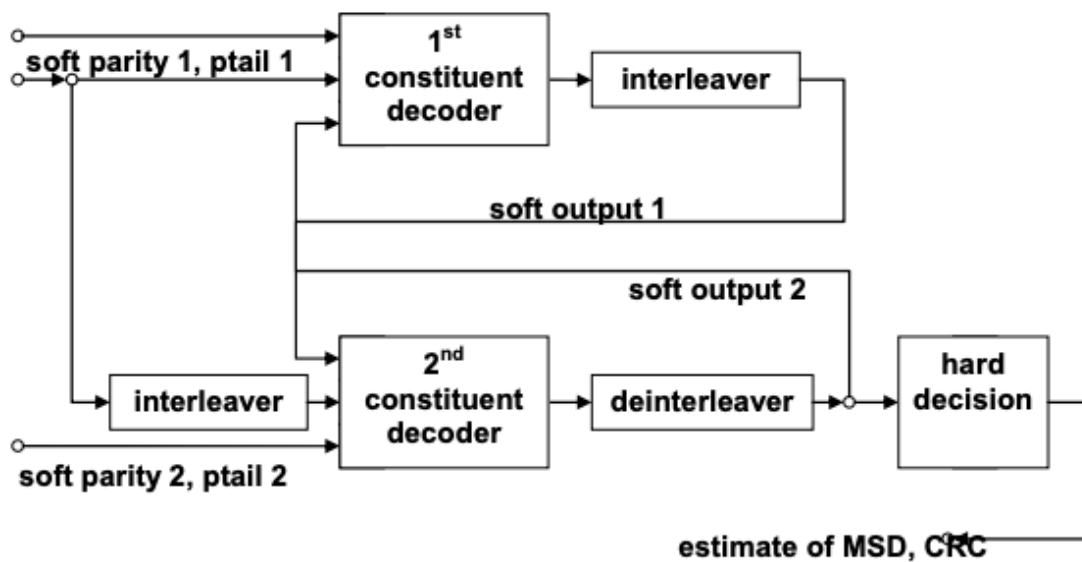


Figure 18: Turbo decoder

(E.g., 3GPP TS 26.267, at 25 (v. 11), 24 (v. 8)). The source code associated with the figure, for example, indicates that it generated soft decision based on the BCJR algorithm. Data processed by the BCJR algorithm was interleaved or deinterleaved, resulting in “soft output 1” or “soft output 2,” respectively, as shown in the figure:

```

/* initialize memory */
Le12 = (IntLLR*)&decBits[0];
Le21 = (IntLLR*)&decBits[sizeof(IntLLR)*(NRB_INFO_CRC + NRB_TAIL)];
memset(Le12, 0, sizeof(IntLLR)*(NRB_INFO_CRC + NRB_TAIL));
memset(Le21, 0, sizeof(IntLLR)*(NRB_INFO_CRC + NRB_TAIL));

/* iterative decoding */
for (i = 0; i < FEC_ITERATIONS; i++) {
    memcpy(Le12, Le21, sizeof(IntLLR)*(NRB_INFO_CRC + NRB_TAIL));

    /* add received systematic bits to extrinsic information */
    for (j = 0; j < NRB_INFO_CRC+NRB_TAIL; j++) {
        temp = (Int32)Le12[j] + (Int32)syst1[j];
        Le12[j] = (ABS(temp) < LLR_MAX) ?
            (IntLLR)temp : (IntLLR)(SIGN(temp)*LLR_MAX);
    }
    /* decode code one (produces Le12) */
    Bcjr(parity1, Le12);

    /* interleave extrinsic information (produces interleaved Le12) */
    Interleave(Le12, Le21);

    /* add received systematic bits to extrinsic information */
    for (j = 0; j < NRB_INFO_CRC; j++) {
        temp = (Int32)Le21[j] + (Int32)syst1[interleaverSeq[j]];
        Le21[j] = (ABS(temp) < LLR_MAX) ?
            (IntLLR)temp : (IntLLR)((SIGN(temp))*LLR_MAX);
    }
    for (j = 0; j < NRB_TAIL; j++) {
        Le21[j+NRB_INFO_CRC] = syst2[j];
    }

    /* decode code two (produces interleaved Le21) */
    Bcjr(parity2, Le21);

    /* deinterleave extrinsic information (produces Le21) */
    Deinterleave(Le21);
}

```

(*E.g., see*, source code release accompanying 3GPP TS 26.268, `ecall_fec.c`, lines 232-268). The BCJR algorithm included a MAP probability algorithm which processed soft input to generate soft decision: “Turbo codes are composed of an interconnection of component codes through interleavers, typically convolutional codes, and their decoders consist of an equal number of component decoders each of which operates on its corresponding codeword and shares information with other component decoders iteratively according to the topology of the encoder. The decoding algorithm in the component decoders is the maximum a-posteriori probability (MAP) algorithm typically implemented in the form known as the Bahl–Cocke–Jelinek–Raviv (BCJR) algorithm. The main advantage of a MAP decoding algorithm over a maximum likelihood decoding algorithm such as the Viterbi algorithm is that it produces optimum soft information which is crucial to the operation of these decoders. The BCJR algorithm was generalized in [S. Benedetto et al., “A Soft-Input Soft-Output Maximum a posteriori (Map) Module to Decode Parallel and Serial Concatenated Codes,” JPL, TDA Progress Report 42-127, Nov. 1996.] into a soft-input soft-output a posteriori probability (SISO-APP) algorithm to be used as a building block for iterative decoding in code networks with generic topologies. The advantages of the SISO-APP algorithm over other forms of the MAP algorithm is that it is independent of the code type (systematic/nonsystematic, recursive/nonrecursive, trellis with multiple edges), and it generates reliability information for code symbols as well as message symbols which makes it applicable irrespective of the concatenation scheme (parallel/serial/hybrid), and hence will be considered in this paper.” *See* Mansour et al., “VLSI Architectures for SISO-APP Decoders,” IEEE Transactions On Very Large Scale Integration (“VLSI”) Systems, Vol. 11, No. 4 (Aug. 2003), at 627, *available at* <http://shanbhag.ece.illinois.edu/publications/mansr-tvlsi-2003-2.pdf>. *See also id.* at 629 (“The decoding problem can now be defined as follows: given a noisy version of  $\underline{c}$  denoted by

$\underline{y} = \Delta(y_1, \dots, y_k, \dots, y_L)$ , find the data sequence  $\underline{u}$ . There are two probabilistic solutions to this decoding problem. Maximum likelihood (ML) decoding determines the most likely connected path  $\underline{s}$  through the trellis that maximizes the probability  $P(\underline{y}|\underline{s})$ . From  $\underline{s}$ , the most likely data sequence  $\underline{u}$  is easily determined using (1). On the other hand, MAP decoding, which we consider here, determines  $\underline{u}$  by estimating each of the symbols  $u_k$  independently using the observations  $\underline{y}$ . The  $k$ th estimated symbol  $u_k$  is the one that maximizes the posterior probability  $P(u_k|\underline{y})$ , and hence the name symbol-by-symbol MAP. The SISO-APP algorithm, a generalized version of the BCJR-APP algorithm [6], is a probabilistic algorithm that solves the MAP decoding problem.”).

36. Upon information and belief, the Accused Instrumentalities weighed and stored soft decision information into the corresponding memory module (e.g., “interleaver” or “deinterleaver”) as shown in the figures below:

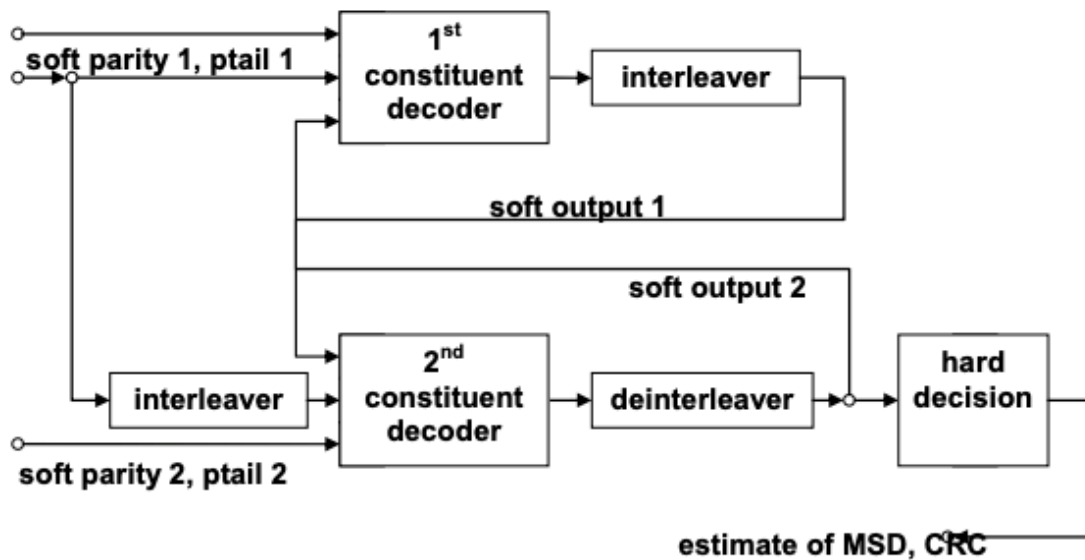


Figure 18: Turbo decoder

(E.g., 3GPP TS 26.267, at 25 (v. 11), 24 (v. 8)). The source code associated with the figure indicates use of the BCJR algorithm as shown below:

```

/* initialize memory */
Le12 = (IntLLR*)&decBits[0];
Le21 = (IntLLR*)&decBits[sizeof(IntLLR)*(NRB_INFO_CRC + NRB_TAIL)];
memset(Le12, 0, sizeof(IntLLR)*(NRB_INFO_CRC + NRB_TAIL));
memset(Le21, 0, sizeof(IntLLR)*(NRB_INFO_CRC + NRB_TAIL));

/* iterative decoding */
for (i = 0; i < FEC_ITERATIONS; i++) {
    memcpy(Le12, Le21, sizeof(IntLLR)*(NRB_INFO_CRC + NRB_TAIL));

    /* add received systematic bits to extrinsic information */
    for (j = 0; j < NRB_INFO_CRC+NRB_TAIL; j++) {
        temp = (Int32)Le12[j] + (Int32)syst1[j];
        Le12[j] = (ABS(temp) < LLR_MAX) ?
            (IntLLR)temp : (IntLLR)(SIGN(temp)*LLR_MAX);
    }
    /* decode code one (produces Le12) */
    Bcjr(parity1, Le12);

    /* interleave extrinsic information (produces interleaved Le12) */
    Interleave(Le12, Le21);

    /* add received systematic bits to extrinsic information */
    for (j = 0; j < NRB_INFO_CRC; j++) {
        temp = (Int32)Le21[j] + (Int32)syst1[interleaverSeq[j]];
        Le21[j] = (ABS(temp) < LLR_MAX) ?
            (IntLLR)temp : (IntLLR)((SIGN(temp))*LLR_MAX);
    }
    for (j = 0; j < NRB_TAIL; j++) {
        Le21[j+NRB_INFO_CRC] = syst2[j];
    }

    /* decode code two (produces interleaved Le21) */
    Bcjr(parity2, Le21);

    /* deinterleave extrinsic information (produces Le21) */
    Deinterleave(Le21);
}

```

(E.g., see, source code release accompanying 3GPP TS 26.268, `ecall_fec.c`, lines 232-268).



```

/* normalization of betaQ */
for (i = 0; i < FEC_STATES; i++) {
temp = (Int32)bTemp1[i] - (Int32)norm;
bTemp1[i] = (temp < (-LLR_MAX)) ? (IntLLR)(-LLR_MAX) : (IntLLR)temp;
}

...

/* normalization of alphaQ */
for (i = 0; i < FEC_STATES; i++) {
temp = (Int32)alpha2[i] - (Int32)norm;
alpha2[i] = (temp < (-LLR_MAX)) ? (IntLLR)(-LLR_MAX) : (IntLLR)temp;
}

```

(E.g., see, source code release accompanying 3GPP TS 26.268, `ecall_fec.c`, lines 318-352). Data processed by the BCJR algorithm, for example, generates soft decision information. “Turbo codes are composed of an interconnection of component codes through interleavers, typically convolutional codes, and their decoders consist of an equal number of component decoders each of which operates on its corresponding codeword and shares information with other component decoders iteratively according to the topology of the encoder. The decoding algorithm in the component decoders is the maximum a-posteriori probability (MAP) algorithm typically implemented in the form known as the Bahl–Cocke–Jelinek–Raviv (BCJR) algorithm. The main advantage of a MAP decoding algorithm over a maximum likelihood decoding algorithm such as the Viterbi algorithm is that it produces optimum soft information which is crucial to the operation of these decoders. The BCJR algorithm was generalized in [S. Benedetto et al., “A Soft-Input Soft-Output Maximum a posteriori (Map) Module to Decode Parallel and Serial Concatenated Codes,” JPL, TDA Progress Report 42-127, Nov. 1996.] into a soft-input soft-output a posteriori probability (SISO-APP) algorithm to be used as a building block for iterative decoding in code networks with generic topologies. The advantages of the SISO-APP algorithm over other forms of

the MAP algorithm is that it is independent of the code type (systematic/nonsystematic, recursive/nonrecursive, trellis with multiple edges), and it generates reliability information for code symbols as well as message symbols which makes it applicable irrespective of the concatenation scheme (parallel/serial/hybrid), and hence will be considered in this paper.” See Mansour et al., “VLSI Architectures for SISO-APP Decoders,” IEEE Transactions On Very Large Scale Integration (“VLSI”) Systems, Vol. 11, No. 4 (Aug. 2003), at 627, *available at* <http://shanbhag.ece.illinois.edu/publications/mansr-tvlsi-2003-2.pdf> (citations removed).

37. As shown by the source code associated with the figure, the soft decision information was then normalized, or “weighted,” and then output to either (1) the “interleaver” memory module if performed at the first soft decision decoder or (2) the “deinterleaver” memory module if performed at the second soft decision decoder shown in the figure. Note that the variables “betaQ” and “alphaQ” comprise examples of such soft decision information in the source code:

```

/* normalization of betaQ */
for (i = 0; i < FEC_STATES; i++) {
temp = (Int32)bTemp1[i] - (Int32)norm;
bTemp1[i] = (temp < (-LLR_MAX)) ? (IntLLR)(-LLR_MAX) : (IntLLR)temp;
}

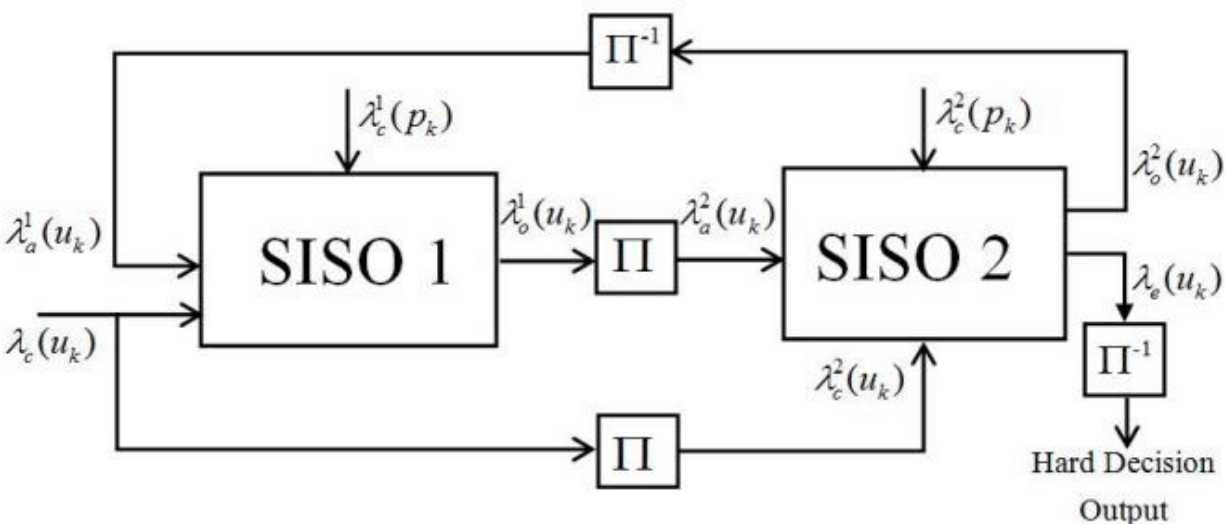
...

/* normalization of alphaQ */
for (i = 0; i < FEC_STATES; i++) {
temp = (Int32)alpha2[i] - (Int32)norm;
alpha2[i] = (temp < (-LLR_MAX)) ? (IntLLR)(-LLR_MAX) : (IntLLR)temp;
}

```

(E.g., see, source code release accompanying 3GPP TS 26.268, `ecall_fec.c`, lines 318-352).

38. Additionally, or alternatively, as explained above, all known commercial implementations of 4G LTE turbo decoders were iterative and functionally equivalent to the figures below. The figures below illustrate that soft decision information was stored in the corresponding memory module (e.g., the a posteriori output of SISO 1 is stored in the associated interleaver memory module  $\Pi$ , while the a posteriori output of SISO 2 is stored in the associated de-interleaver memory module  $\Pi^{-1}$ )



See Jun Li et al., "Turbo Decoder Design based on an LUT-Normalized Log-MAP Algorithm," Entropy (Basel) (Aug. 20, 2019), available at <https://www.ncbi.nlm.nih.gov/pmc/articles/PMC7515343/>.

39. On information and belief, use of any viable maximum a posteriori (MAP) probability algorithm and/or logarithm approximation algorithm necessarily required weighing (or "normalization"). See Jun Li et al., "Turbo Decoder Design based on an LUT-Normalized Log-MAP Algorithm," Entropy (Basel) (Aug. 20, 2019), available at <https://www.ncbi.nlm.nih.gov/pmc/articles/PMC7515343/> (discussing use of a log maximum a posteriori decoding algorithm). See also, e.g., Guohui Wang et al., "High-throughput Contention-Free Concurrent Interleaver Architecture for Multi-standard Turbo Decoder," ASAP 2011—22nd

IEEE International Conference on Application-specific Systems, Architectures and Processors 113 (Sept. 2011) (noting that MAP decoders are used as the component SISO decoders); Cristian Anghel et al., “CTC Turbo Decoding Architecture for LTE Systems Implemented on FPGA,” ICN 2012: The Eleventh International Conference on Networks 199, 200 (2012) (describing ideal use of classic MAP algorithm and practical implementation of log-MAP algorithms).

40. The Accused Instrumentalities performed, for a predetermined number of times, iterative decoding from the first to the last of multiple decoders, wherein an output from the last soft decision decoder was fed back as an input to the first soft decision decoder, then from the first to the second decoders, and propagated to the last decoder in a circular circuit, as shown in the figures below:

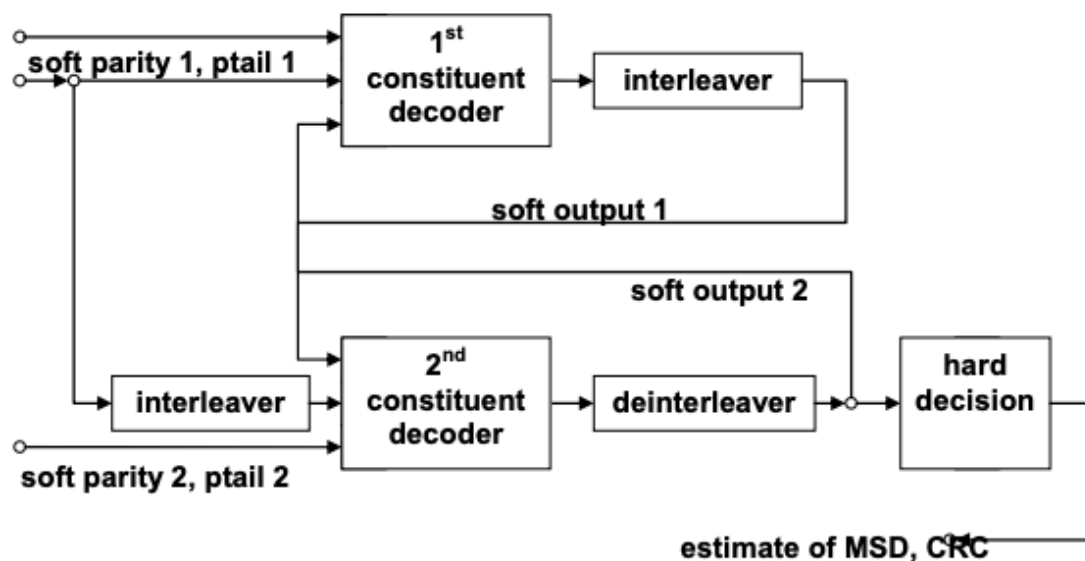


Figure 18: Turbo decoder

(E.g., 3GPP TS 26.267, at 25 (v. 11), 24 (v. 8)). As shown in the example figure, decoding occurred from the first soft decision decoder, “1<sup>st</sup> constituent decoder,” to the second, or last, soft decision decoder, “2<sup>nd</sup> constituent decoder.” The second soft decision decoder outputs “soft output 2,” which is fed as back as an input to the first soft decision decoder. The first soft decision

decoder outputs “soft output 1.” This “soft output 1” is fed as input into the second soft decision decoder. The second soft decision decoder is the last soft decision decoder in a circular circuit propagating from the first soft decision decoder to the second soft decision decoder to the first ... to the second to the first to the second, etc. This process was performed a predetermined number of times as defined by the software governing the turbo decoding process. For example, the default number of iterations defined in the source code associated with the figure is 8 iterations, stored in the variable FEC\_ITERATIONS:

```
#define FEC_VAR          (30206)          variance: 1/4550000 in Q37
#define FEC_MEAN        (0xB9999A)      mean: 5.8 in Q21
#define FEC_ITERATIONS  (8)             number of decoder iterations
#define FEC_STATES      (8)             number of decoder states
```

(*E.g.*, 3GPP TS 26.267, at 25 (v. 11), 24 (v. 8)). As another example, FEC\_ITERATIONS is used during decoding process:

```

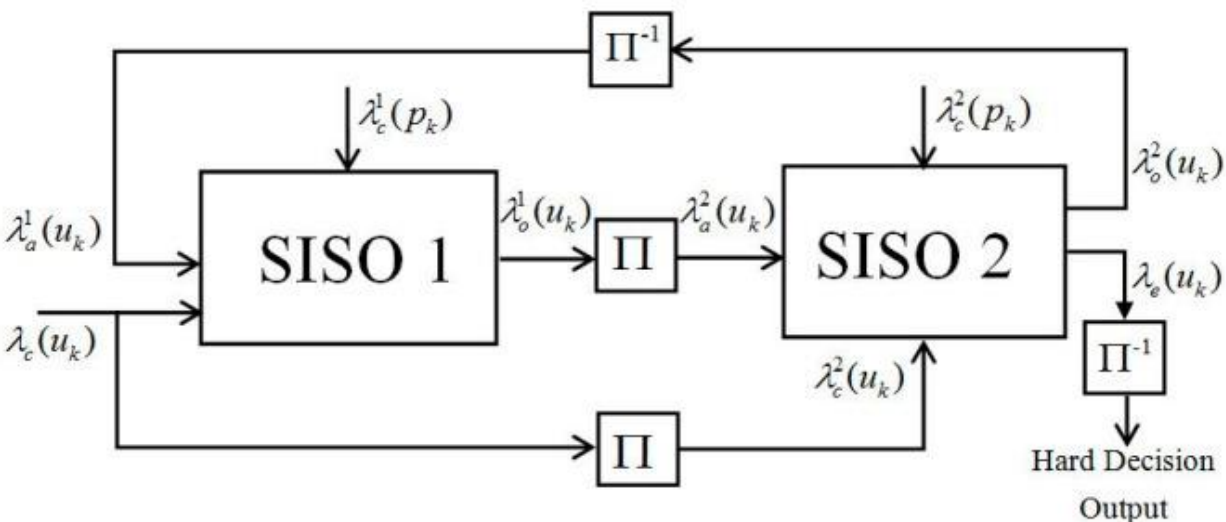
/* iterative decoding */
for (i = 0; i < FEC ITERATIONS; i++) {
  memcpy(Le12, Le21, sizeof(IntLLR)*(NRB_INFO_CRC + NRB_TAIL));
  /* add received systematic bits to extrinsic information */
  for (j = 0; j < NRB_INFO_CRC+NRB_TAIL; j++) {
    temp = (Int32)Le12[j] + (Int32)syst1[j];
    Le12[j] = (ABS(temp) < LLR_MAX) ?
              (IntLLR)temp : (IntLLR)(SIGN(temp)*LLR_MAX);
  }
  /* decode code one (produces Le12) */
  Bcjr(parity1, Le12);
  /* interleave extrinsic information (produces interleaved Le12) */
  Interleave(Le12, Le21);
  /* add received systematic bits to extrinsic information */
  for (j = 0; j < NRB_INFO_CRC; j++) {
    temp = (Int32)Le21[j] + (Int32)syst1[interleaverSeq[j]];
    Le21[j] = (ABS(temp) < LLR_MAX) ?
              (IntLLR)temp : (IntLLR)((SIGN(temp))*LLR_MAX);
  }
  for (j = 0; j < NRB_TAIL; j++) {
    Le21[j+NRB_INFO_CRC] = syst2[j];
  }
  /* decode code two (produces interleaved Le21) */
  Bcjr(parity2, Le21);
  /* deinterleave extrinsic information (produces Le21) */
  Deinterleave(Le21);
}

```

(E.g., see, source code release accompanying 3GPP TS 26.268, ecall\_fec.c, lines 232-268).

41. Additionally, or alternatively, as above, all known commercial implementations of 4G LTE turbo decoders were iterative and functionally equivalent to the figures below. The figures below illustrates an output from the last soft decision decoder was fed back as an input to the first soft decision decoder, then from the first to the second decoders, and propagate to the last decoder in a circular circuit (e.g., the a posteriori output of SISO 2 is de-interleaved with the associated

memory module and fed as a priori input of SISO 1, while the a posteriori output of SISO 1 is interleaved with the associated memory module and fed as a priori input of SISO 2).



(E.g., Jun Li et al., "Turbo Decoder Design based on an LUT-Normalized Log-MAP Algorithm," Entropy (Basel) (Aug. 20, 2019), available at <https://www.ncbi.nlm.nih.gov/pmc/articles/PMC7515343/>). Iterative turbo decoder implementations required completing a certain number of iterations to complete decoding a frame with a satisfactory degree of confidence. Iterative decoding must have therefore been performed a predetermined number of times according to a stopping rule. See, e.g., A. Matache et al., "Stopping Rules for Turbo Decoders," TMO Progress Report 42-142 (Aug. 15, 2000), available at [https://ipnpr.jpl.nasa.gov/progress\\_report/42-142/142J.pdf](https://ipnpr.jpl.nasa.gov/progress_report/42-142/142J.pdf).

42. Upon information and belief, Defendant was indirectly infringing by way of inducing infringement and contributing to the infringement of the asserted claim of the '742 Patent in the State of Texas, in this District, and elsewhere in the United States, by providing the Accused Instrumentalities for use as described above by Defendant's customers. Defendant advertised, offered for sale, and/or sold the Accused Instrumentalities to its customers for use in a manner that Defendant knew infringed at least one claim of the '742 Patent. For example, Defendant sold the

Accused Instrumentalities advertising that the products operated using 3G and/or 4G-LTE. Defendant was a direct and indirect infringer, and its customers using the Accused Instrumentalities were direct infringers. Defendant had actual knowledge of the '742 Patent at least as early as when they received a letter from Plaintiff sent on October 18, 2021, asserting that the use of the Accused Instrumentalities infringed claims of the '742 Patent and they were provided a chart of the infringement. Defendant has known of its infringement since at least that date as a result of the accusations of infringement in the letter. Defendant has therefore also known that the use of the Accused Instrumentalities by its customers infringed at least one claim of the '742 Patent since at least the date they received the letter.

43. On information and belief, since becoming aware of the '742 Patent and of the infringement through advertising and offering for sale the Accused Instrumentalities for use by its customers, Defendant was committing the act of inducing infringement by specifically intending to induce infringement by providing the Accused Instrumentalities to its customers and by aiding and abetting its use in a manner known to infringe by Defendant. Since becoming aware of the infringing use of the Accused Instrumentalities, Defendant knew that the use of the Accused Instrumentalities by its customers for a method of iteratively decoding a plurality of sequences of received baseband signals as described in claim 6 constituted direct patent infringement. Despite this knowledge, Defendant continued to encourage and induce its customers to use the Accused Instrumentalities to infringe as described above and provided instructions for using the Accused Instrumentalities to infringe, including through advertisements. Defendant therefore knowingly induced infringement and specifically intended to encourage and induce the infringement of the '742 Patent by its customers.



44. On information and belief, since Defendant became aware of the infringement at least as of the date of receipt of the letter, Defendant committed the act of contributory infringement by intending to provide the identified Accused Instrumentalities to its customers knowing that it was a material part of the invention, knowing that its use was made and adapted for infringement of the '742 Patent as described above, and further knowing that the accused aspect of the Accused Instrumentalities described above were not a staple article or commodity of commerce suitable for substantially noninfringing use. As described above, Defendant was aware that all material claim limitations were satisfied by the use and implementation of the Accused Instrumentalities by Defendant's customers in the manner described above yet continued to provide the Accused Instrumentalities to its customers knowing that it was a material part of the invention. As described above, since learning of the infringement, Defendant knew that the use and implementation of the Accused Instrumentalities by its customers was made and adapted for infringement of the '742 Patent. A new act of direct infringement occurred each time a customer implemented and/or used the Accused Instrumentalities in the manner described above. After Defendant became aware that the use of the Accused Instrumentalities infringed at least one claim of the '742 Patent, Defendant knew that each such new use was made and adapted for infringement of at least one claim of the '742 Patent and Defendant continued to advertise and provide the Accused Instrumentalities for such infringing activities. Furthermore, as described more fully above, the Accused Instrumentalities had functionality designed for use in the system in the manner described above and was therefore not a staple article or commodity of commerce suitable for substantially noninfringing use.

45. Upon information and belief, Defendant was willfully infringing the asserted claim of the '742 Patent in the State of Texas, in this District, and elsewhere in the United States. As

explained above, Defendant was informed of its infringement of the '742 Patent by way of the October 18, 2021, letter sent to Defendant, including a claim chart demonstrating Defendant's infringement. As a result of the letter, Defendant should have known that its actions constituted an unjustifiably high risk of infringement. Despite the letter and knowledge that the risk of infringement was either known or so obvious that it should have been known, Defendant continued its infringing actions.

46. Plaintiff has been damaged as a result of Defendant's infringing conduct. Defendant is thus liable to Plaintiff for damages in an amount that adequately compensates Plaintiff for such Defendant's infringement of the '742 Patent, *i.e.*, in an amount that by law cannot be less than would constitute a reasonable royalty for the use of the patented technology, together with interest and costs as fixed by this Court under 35 U.S.C. § 284.

#### **IV. JURY DEMAND**

Plaintiff, under Rule 38 of the Federal Rules of Civil Procedure, requests a trial by jury of any issues so triable by right.

#### **V. PRAYER FOR RELIEF**

WHEREFORE, Plaintiff respectfully requests that the Court find in its favor and against Defendant, and that the Court grant Plaintiff the following relief:

- a. Judgment that one or more claims of United States Patent No. 6,813,742 have been infringed, either literally and/or under the doctrine of equivalents, by Defendant;
- b. Judgment that Defendant account for and pay to Plaintiff all damages to and costs incurred by Plaintiff because of Defendant's infringing activities and other conduct complained of herein;
- c. Adjudging that Defendant's infringement of the '742 Patent was willful and trebling all damages awarded to Turbocode for such infringement pursuant to 35 U.S.C. § 284;

- c. That Plaintiff be granted pre-judgment and post-judgment interest on the damages caused by Defendant's infringing activities and other conduct complained of herein; and
- d. That Plaintiff be granted such other and further relief as the Court may deem just and proper under the circumstances.

August 30, 2024

DIRECTION IP LAW

/s/ David R. Bennett

David R. Bennett (IL Bar No.: 6244214)

P.O. Box 14184

Chicago, Illinois 60614-0184

Telephone: (312) 291-1667

dbennett@directionip.com

*Attorneys for Plaintiff TurboCode LLC*